Hydrogel-Based Flexible Electronics

Lixuan Hu[1], Pei Lin Chee[2], Sigit Sugiarto[2], Yong Yu[2], Chuanqian Shi[4], Ren Yan[1], Zhuoqi Yao[1], Xuewen Shi[1], Jiacai Zhi[1], Dan Kai[2,3]*, Hai-Dong Yu[1]*, Wei Huang[1]*

[1] Frontiers Science Center for Flexible Electronics, Xi'an Institute of Flexible Electronics (IFE) and Xi'an Institute of Biomedical Materials & Engineering, Northwestern Polytechnical University, 127 West Youyi Road, Xi'an 710072, PR China. E-mail: iamwhuang@nwpu.edu.cn

[2]Institute of Materials Research and Engineering (IMRE), A∗STAR, 2 Fusionopolis Way, Innovis, No. 08-03, Singapore, 138634, Singapore

[3]Institute of Sustainability for Chemicals, Energy and Environment (ISCE2), A∗STAR, 2 Fusionopolis Way, Innovis, No. 08-03, Singapore, 138634, Singapore

[4]School of Aerospace Engineering and Applied Mechanics, Tongji University, Shanghai 200092, PR China.

Abstract

Flexible electronics is an emerging field of research involving multiple disciplines, which include but not limited to physics, chemistry, materials science, electronic engineering, and biology. However, the broad applications of flexible electronics are still restricted due to several limitations, including high Young's modulus, poor biocompatibility, and poor responsiveness. Innovative materials aiming for overcoming these drawbacks and boost its practical application is highly desirable. Hydrogel is a class of 3D crosslinked hydrated polymer networks, and its exceptional material properties render it a promising candidate for the next generation of flexible electronics. Here, we review the latest methods of synthesizing advanced functional hydrogels and the state-of-art applications of hydrogel-based flexible electronics in various fields. More importantly, we discuss on the correlation between properties of the hydrogel and device performance, to have better understanding of the development of flexible electronics by using environmentally responsive hydrogels. Lastly, we provide perspectives on the current challenges and future directions in the development of hydrogel-based multifunctional flexible electronics.

Keywords: bio-electronic interface, hydrogel artificial skin, wearable devices, soft integrated electronics, hydrogel machines

1. Introduction

Flexible electronics refer to circuits and electronic components that can maintain their functions under circumstances of bending, rolling, folding, or stretching.[1] The concept of flexible electronics was coined in the 1960s when thin and flexible solar cells with higher power density were designed for satellites.[2] Ever since then, innovations in materials with greater flexibility and large processability, such as conductive polymers[3], organic semiconductors,[4,5] and amorphous silicon,[6] have gradually laid the foundation for flexible electronics. In recent years, there is an increase in popularity on the research for new materials and fabrication techniques that incorporate high performance electronic components directly onto flexible substrates. Applications of flexible electronics have been greatly expanded, which include flexible sensors,[7-9] flexible energy harvesting devices,[10-12] flexible energy storage devices,[13,14] flexible transistors,[15-17] and flexible display screens[18,19]. Some of these applications have already been commercialized and made their way into people's lives (e.g., flexible display screens and flexible solar cells). In comparison to the more rigid and tough traditional electronic devices, flexible electronic devices possess some unique advantages, such as light weight, portability, great flexibility, bendability, foldability, and adaptability which are desirable for many diverse applications.[20] More recently, technology advances in artificial intelligence, cloud computing, augmented reality, and virtual reality, along with the ever-increasing awareness of personal health management have catalyzed the emergence of flexible electronics interfacing the living biological tissues and synthetic electronic systems (the so-called bio-electronics or bio-integrated wearable systems).[21-23]

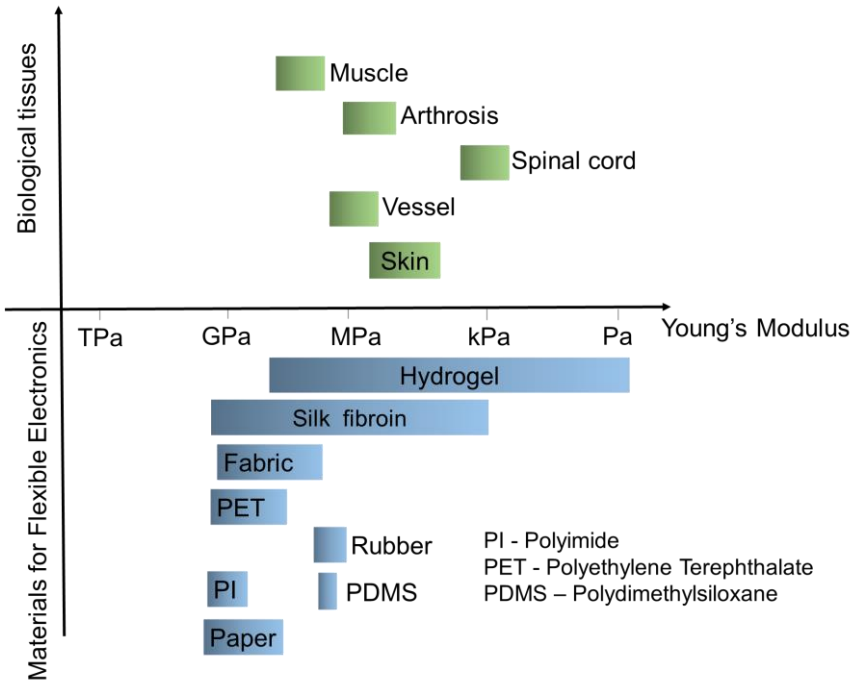

Figure 1. Young's moduli of biological tissues (highlighted in green), common flexible electronics materials (highlighted in blue), and hydrogels.

One of the major drawbacks in the development of bioelectronics is the stark dissimilarity between conventional electronics and biological tissues. The human body is made up of a series of soft, water-rich tissues, and organs mostly with Young's moduli of several kilopascals to tens of megapascals (Figure 1). A wide range of synthetic polymers (e.g., PI, PET, rubber, silicone, etc.) which has potential to be used as substrates for flexible electronics, however, they either have too large Young's moduli (gigapascals) or lack in adequate biocompatibility.[18] Hydrogel is a promising candidate for the development of flexible electronics, especially for biological applications as they closely mimic the mechanical, chemical, and optical properties of the biological tissues. Hydrophilic crosslinked polymer hydrogels have high-water contents, thus behaving as both a solid and a liquid.[24-26] They are intrinsically soft, highly bendable, stretchable, and possess self-healing properties due to their versatility in mechanical and bio-functional engineering.[27] As a result, hydrogel-based flexible electronics can have better conformability and affinity with biological tissues and organisms. These advantageous

characteristics allow hydrogel-based flexible electronics to outperform commercially available biological electronic components[28] which are generally rigid, dry, or are not compatible enough to bind to human tissues.[24,29]

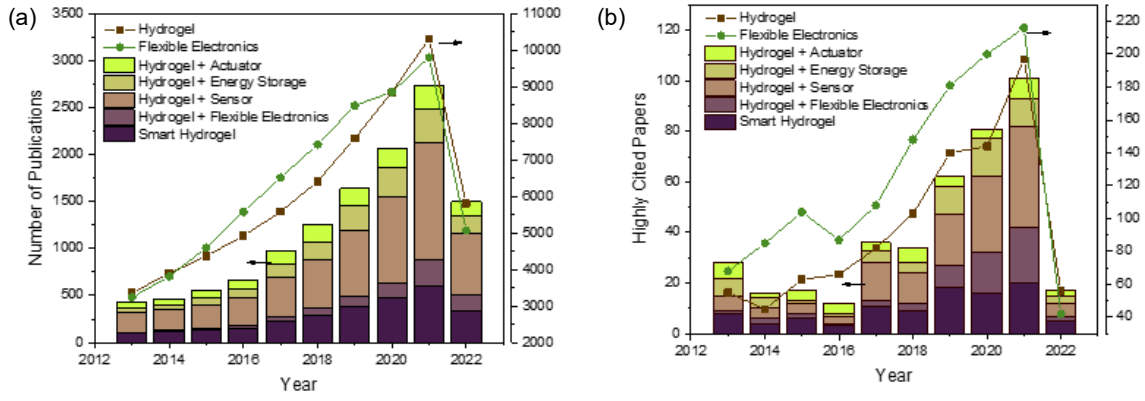

Figure 2. (a) Total number of publications and (b) highly cited articles related to hydrogel-based flexible electronics in the last 10 years. According to Web of Science, searched on 1 August 2022.

Within the last 10 years, there has been an increasing research interests in the development of hydrogel-based flexible electronics driven by secular trends in digitalization and improving awareness of personal health and lifestyle. Figure 2 highlights the ever-increasing total number of research (a) and highly cited articles (b) on hydrogel-based flexible electronics published in the past ten years. Notably, we have witnessed the total number of publications on hydrogel and flexible electronics each tripled from 2013 to 2021 with the number of highly cited articles on respective topics growing at a similar pace (dotted lines). More rigorous inspection identifies actuators, sensors, energy storage devices, and smart hydrogels among the hottest topics of hydrogel-based flexible electronics (bar graphs). Several reviews have been published in the field relevant to hydrogel-based flexible electronics. For instance, Zhao *et al.* have reviewed the potential of using hydrogel as machines, such as hydrogel coatings, hydrogel optics, *etc.*, but the review has limited context to electronics.[24] Wang *et al.* have published a comprehensive review on the design and preparation of conductive hydrogels used in super-

capacitors.[30] This review mainly focused on improving the conductivity of hydrogels and did not elaborate on the application of hydrogel flexible electronics apart from super-capacitors. Guo *et* al. comprehensively reviewed the design, properties and applications of stimuli-responsive conductive hydrogels. [31] In contrast to previous reviews, herein we focus on the synthesis of functionalized hydrogels tailored to their diverse applications as flexible electronics. In this work, we first provide a well-rounded introduction to hydrogels and describe the latest strategies and approaches to engineer functional hydrogels. We then summarize various state-of-art applications of hydrogel-based flexible electronics, ranging from sensors and actuators to energy harvesting and storage devices, to electromagnetic shielding devices, and to drug control release devices (Figure 3). Finally, we provide perspectives on current challenges and future development of multifunctional hydrogel-based flexible electronics. Particularly, various approaches to boost the function and applications of hydrogel-based flexible electronics are presented, which will hopefully provide an overview for designing hydrogels with desired properties and provide insights to the prospective applications of hydrogel-based flexible electronics in general.

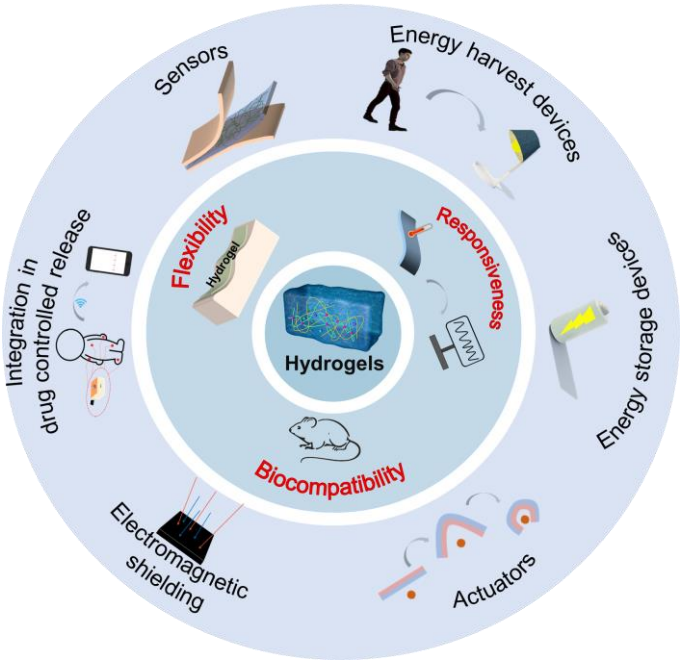

Figure 3. Main features of hydrogels and their applications in flexible electronics.

2. Overview of Hydrogels

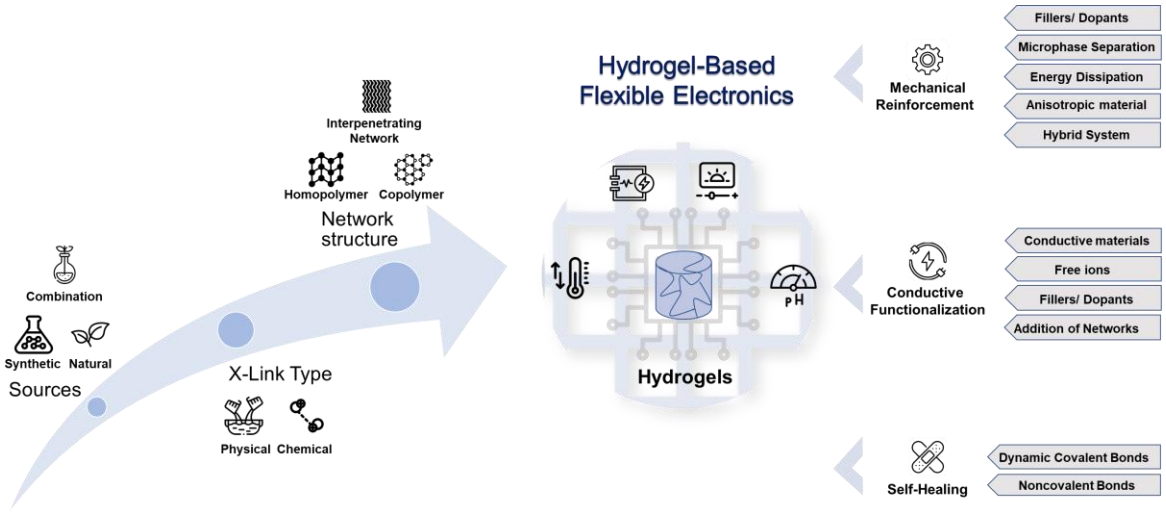

Figure 4. Overview of hydrogels and approaches to boost their functions for hydrogel-based flexible electronics.

Hydrogels are defined as a 3D network of polymers that can store and retain a significant amount of fluid within their own structure known as swelling. This swelling behavior arises from the chemical or physical crosslinking of the polymer chains that hold and maintain the network structure. Hydrogels can be divided into several classifications depending on the type of crosslinking (physical or chemical), source of polymer (polymer, synthetic, and hybrid), and network structure (homopolymeric, copolymeric, and interpenetrating) as summarized in Figure 4.

2.1. Source of Polymer

Hydrogels can be synthesized with either natural polymer source, synthetic source, or a combination of both. Natural hydrogels are synthesized from polymers that are obtained from natural sources such as plants or animals. Some common examples of natural polymers include cellulose, alginate, chitosan, and gelatin.[32] Tang *et al.* prepared a microfluidic pH sensor using

chitosan hydrogel for rapid detection of antibiotic sensitivity.[33] The whole bacterial growth curve can be obtained in less than 2 h. Synthetic hydrogels, as the name suggests, are of those that are synthesized from synthetic polymer formed by chemical polymerization methods such as polyethylene glycol (PEG), polylactic acid (PLA), polycaprolactone (PCL), and polyvinyl alcohol (PVA).[32] In the context of biomaterials, a combination of both natural and synthetic sources can be used to form hybrid hydrogels to optimize both the mechanical and chemical properties alongside with the biocompatibility and biodegradability.[34] Ren *et al.* developed a hydrogel sensor based on O-carboxyl chitosan and PVA. The hydrogel sensor exhibited biocompatibility, good antibacterial property, and stretchability.[35] Jiang *et al*. developed a new hybrid hydrogel system with glycerol-modified PVA that has been reinforced by 3D printed PCL-graphene composite scaffold.[36] The newly formed hydrogel had excellent mechanical properties that mimics natural load-bearing cartilage.

2.2. Crosslinking of Hydrogels

Hydrogels can be prepared by either physical or chemical crosslinking. Physical crosslinking relies on intermolecular reversible interactions such as hydrogen bonds, electrostatic interactions, entanglements, hydrophobic or hydrophilic interactions, metal coordination, and π–π stacking.[37] A physically crosslinked hydrogel can benefit from being able to respond to external stimulus such as pH or temperature changes, this enables them to have useful properties such as self-healing and injectable in ambient temperatures. Furthermore, such physical crosslinking can be cleaved in physiological conditions, thereby providing the hydrogels with good biodegradability. However, they typically have lower mechanical strength due to the weaker intermolecular interactions.

Chemical crosslinking involves formation of stronger and permanent bonds that form linkages between polymer chains, often in a form of covalent bonds. Some of the common crosslinking

methods include free radical polymerization, grafting, and Schiff base formation.[38] Due to the formation of permanent and stable bonds, chemically crosslinked hydrogel would have a better mechanical properties and stability under physiological conditions. Ye *et al*. managed to improve the mechanical properties of cellulose hydrogels by chemically dual-crosslinking cellulose hydrogels (DCH) using both high and low molecular weight crosslinkers.[39] The DCH were able to show pristine strength and toughness which is an advantage over conventional hydrogels. This work has shown a good prospect on the development on sustainable and dense hydrogel with favorable mechanical properties.[39]

2.3. The Network Structures of Hydrogels

There are three main types of hydrogel network structures: homopolymeric hydrogels, copolymeric hydrogels, and interpenetrating hydrogels.

Homopolymeric hydrogels are synthesized from only one type of monomer. Crosslinked homopolymers have important applications in controlled drug delivery, some examples of these homopolymeric hydrogels include polyethylene glycol (PEG), 2-hydroxyethyl methacrylate (HEMA), and poly(2-hydroxyethyl methacrylate) (PHEMA).[40] There are also uncrosslinked homopolymers that are water-soluble that are utilized in the biomedical and agricultural applications.[41] On the other hand, copolymeric hydrogels are covalently or ionically crosslinked polymers that are synthesized from two or more different kinds of monomers that are arranged in a random, block, or alternating configuration, which consist of at least one hydrophilic component.

Interpenetrating network (IPN) hydrogels are composed of two independent crosslinked polymers that are contained and interlaced within a network which increases the mechanical strength of the hydrogel. A semi-IPN are IPN in which one of the component is crosslinked, while the other is an uncrosslinked polymer.[42] One of the most important aspect to IPNs is

that each polymeric network component is able to retain its own property while having the flexibility to alter the composition ratio of the polymer components to adjust the combined properties of the components in the IPN.[43] These hydrogels are useful in the area of cell culturing scaffolds for tissue engineering.[44] In recent work, Ren *et al*. developed physically crosslinked and interpenetrating double network hydrogels using poly (vinyl alcohol) (PVA) and fish gelatin (FG).[45] These hydrogels were loaded with salicylic acid for its antibacterial properties. They successfully showed that the newly formed hydrogels possessed good physical properties and able to perform well in sustained drug release, which is desirable for medical applications such as wound dressing. Censi *et al*. synthesized an interpenetrating hydrogel network using a covalent network of vinyl sulfone triblock copolymers with tandem crosslinking by thermal gelation and Michael addition with thiolated hyaluronic acid, and a network of crosslinked fibrin. The resulting IPN hydrogel showed a good storage modulus and significant increase in degradation time. [46] These IPN hydrogels are also useful in the area of sensors for detection of physiological signals. Ye *et al.* prepared an interpenetrating polymer network of multiwalled carbon nanotube-poly(3,4-ethylenedioxythiophene)/ poly(styrenesulfonate)-polyacrylamide-poly (vinyl alcohol)/ borax composite hydrogel cross-linked in a simplified process. The hydrogel offers injectable, high tensile, electrically conductive, and adhesive properties. The hydrogel can realize reliable detection of physiological signals.[47]

2.4. Types of "Smart" Hydrogels

Hydrophilic crosslinked polymer hydrogels have high-water contents, thus behaving as both a solid and a liquid.[24-26] They are intrinsically soft, highly bendable, stretchable, and possess self-healing properties due to their versatility in mechanical and bio-functional engineering.[27] Recently, there are a group of hydrogels reported that are able to be responsive to various external stimuli such as temperature, light, electrical field, and pH, known as "smart" materials.

This makes hydrogels to be an excellent candidate for various biomedical and hydrogel-based flexible electronics applications.

2.4.1. Response to Temperature

A popular class of hydrogels that is temperature-sensitive is often known as thermogels. Most polymers will dissolve more easily with increasing temperature. However, there are some polymers that decreases in water solubility with increasing temperature exhibit a phase transition at certain temperature known as the lower critical solution temperature (LCST). Below the LCST, such polymers dissolve well in water due to hydrogen bonding between the polymers and water. Above the LCST, these hydrogen bonds are broken, and the polymer chains collapse and precipitate out of the water forming a cloudy solution. Due to this behavior, thermogels swells in temperatures below the LCST and collapse above the LCST[48] This allows thermogels to be particularly useful in the field of controlled drug release. Zheng *et al*. synthesized a multiblock poly (ether ester urethane) and studied the drug release properties using paclitaxel and doxorubicin as model drugs.[49] It was shown that the thermogel was able to sustain a controlled release over two weeks and able to inhibit the growth of tumour. Another interesting potential application of thermogel is to absorb moisture from air and controllably release the trapped water with temperature changes (Figure 5). This work was done by Matsumoto *et al*. where they developed a thermo-responsive IPN comprising of poly(N-isopropylacrylamide) and sodium alginate in the dry state.[50] Their work showed that the thermogel was able to absorb considerable amount of moisture from the air at temperatures below the LCST, and to squeeze out the absorbed moisture at temperatures above the LCST. This work opened up the possibility to use thermo-responsive hydrogel for water exchange system with low energy consumption. Luo *et al.* designed a deformable ion electrode based on a physically cross-linked thermogel, which gradually changed from a viscous liquid to a viscoelastic gel, which locks the deformable electrode with an irregular surface, and established

a conformal interface.[51]

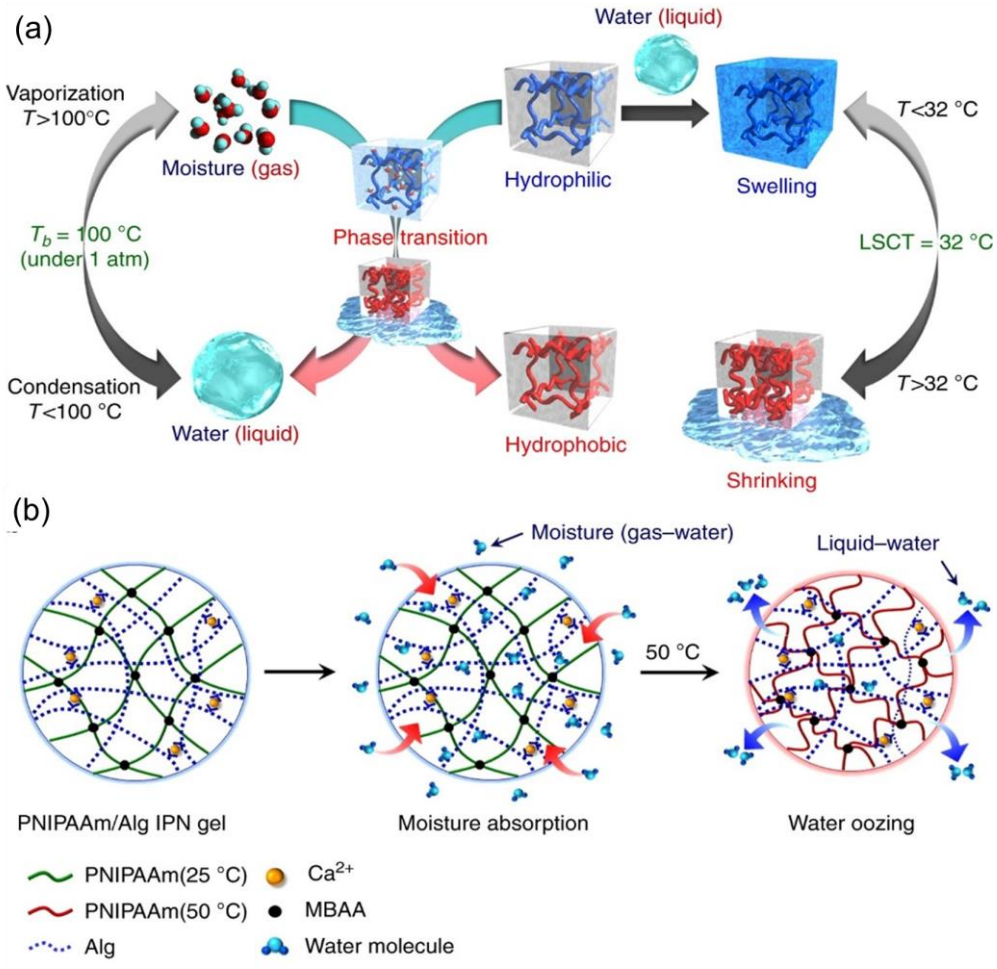

Figure 5. Conceptual illustration of the temperature transition study. (a) Water-adsorption and desorption of dried PNIPAAm/Alg IPN gel. (b) Moisture absorption and desorption of IPN gels at different temperature. Reproduced with permission from Nature.[50] Copyright 2018.

2.4.2. Response to Light

Photo-responsive hydrogels respond to light radiation of suitable wavelengths. The light radiation affects the polymer through changes that occur on specific functional groups upon exposure. These changes include hydrogel formation or degradation, swelling or shrinking of the polymer network, and chemical modifications within the network.[52] The work around photo-responsive hydrogels are particularly interesting due their potential use in non-invasive treatment and remote manipulation which is desirable in applications such as controlled drug

delivery.[53] Recently, Pang *et al.* established a smart flexible electronic integrated wound dressing based on UV-responsive antibacterial hydrogel. It can be used for real-time monitoring and on-demand treatment of infected wounds.[54] Another potential application of photo-responsive hydrogels was done by Liu and her team. They synthesized a new photo-responsive poly [2-((4,5-dimethoxy-2-nitrobenzyl) oxy)-N-(2-(methacryloyloxy)ethyl)-N,N-dimethyl-2-oxoethan-1-aminium] (polyCBNA) hydrogel that was initially cationic and able to effectively kill bacteria. Under UV irradiation, this hydrogel switched to the zwitterionic form and release the attached bacteria. This work showed the potential use of such hydrogels for self-sterilizing and self-cleaning coating for implants, cell harvesting, and cell patterning.[55]

2.4.3. Response to Electrical Field

Hydrogels have varying electrical charges within its polymer network. According to the charge type, they can be grouped into four different classes: neutral, ionic (contain cationic or anionic), amphoteric (both acidic and basic groups), and zwitterionic (contain both anionic and cationic groups). The different charge types of the respective hydrogel lead to various interesting applications, such as sustained drug delivery,[56] protein absorption,[57] and swelling behavior.[58]

Electro-sensitive hydrogels swell and shrinks under an applied electric field. This class of hydrogels is composed of charged polymers. In an applied electric field, a force is generated between the immobile charged group within the polymeric network and its counterions. The hydrogels are then able to regionally swell or shrink at the respective anode or cathode.[59] The difference in the ionic concentration in the hydrogel polymer network and its medium causes the hydrogel to “bend”. The ability of these electro-sensitive hydrogels to convert electrical energy to mechanical energy had stimulated the research interests of many research groups to manipulate this property for applications in biosensors, drug-delivery, and flexible electronics. Jiang *et al*. developed nanocomposite hydrogel actuator that had high mechanical tensile strength (2 MPa) and automatic bidirectional bending capability with electrical stimulus

(Figure 6).[60] The formed hydrogel was reported to be able to bend in both directions. The direction and extent of bending can be tuned by the variation of the concentration of cations and anions within the gel network. This work showed a potential in the use for soft robotics, artificial muscles, and tissue engineering.

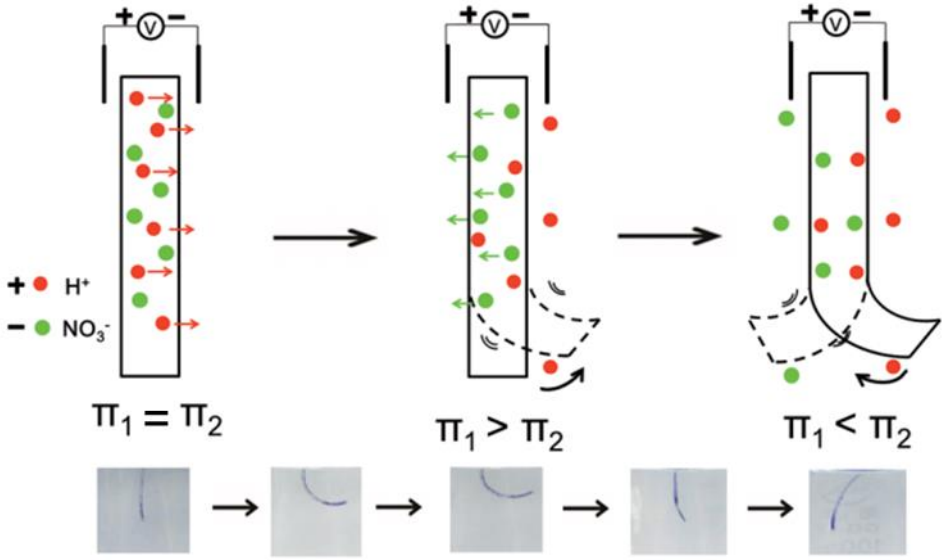

Figure 6. The mechanism of electro-induced bidirectional bending behaviors of the nanocomposite hydrogel. Reproduced with permission from RSC Publications.[60] Copyright 2019.

2.4.4. Response to pH

pH sensitive hydrogels responding to pH changes of the system are able to expand or contract depending on the pH of the medium. This class of hydrogel contain weakly acidic or basic group in the backbone polymer which can be more ionized in higher or lower pH, respectively. The swelling property can be attributed to the electrostatic repulsion of the ionized group.[61] A promising work by Han *et al*. showed the ability of hydrogels that are able to release lipophilic drug based on dual pH-responsive switch. The group made a double-layered structure using two different pH-responsive hydrogels, polyacrylamide (PAAm) hydrogel and polyacrylic acid (PAAc) hydrogel, which were tested to have different swelling ratio at different pH. They have

demonstrated the capability of this dual pH-responsive actuator to release hydrophilic or lipophilic drugs based on the pH of the medium, meantime prevent degradation, metabolism, and excretion of drugs before release.[62] Wang *et al.* designed a conductive hydrogel based on the copolymer network of acrylic acid and hydroxyethyl acrylate doped with graphene oxide.[63] A highly sensitive flexible sensor for monitoring human motion was fabricated using the flexible pH-responsive conductive hydrogel. At the same time, it is combined with the temperature stimulus response hydrogel to detect the environment temperature and realize intelligent control.

3. Approaches to Boost Hydrogel Functions

3.1. Conductive Functionalization

With the recent interests in developing wearable sensors, there is of significant value to understand the available techniques to equip hydrogels with conductive function. In general, the methods can be divided into four broad categories, namely the inclusion of conductive fillers/dopants, the selective use of conductive materials, the introduction of free ions and the addition of a new network.

Conductive-enhancing fillers or dopants is one of the first options that was explored to achieve conductive hydrogels. The preparation is facile with only an additional step of mixing fillers and dopants into the hydrogel components. For instance, Yang *et al.* added sulfonated carbon nanotubes, the conductive fillers, to 2,2,6,6-tetramethylpiperidinyl-1-oxyl (TEMPO)-oxidized cellulose nanofibers before introducing calcium chloride solution to trigger the formation of the conductive hydrogel.[64] Another commonly used filler is graphene which has high charge carrier density and mobility. Its electrical conductivity can reach up to 6×10^5 S m^{-1}.[65] In a recent study, exfoliated graphene was introduced in the form of micro-engineered framework

structures to equip polyacrylamide hydrogels with conductivity. The preparation was different from the usual practice of mixing filler into the hydrogel components. With the aim to minimize the filler effect on the mechanical properties of the hydrogel, a template was used to guide the formation of the exfoliated graphene microstructures. The hydrogel precursor was subsequently introduced to fill the volume unoccupied by the exfoliated graphene. While its presence was in the microscale, the effect of graphene was not negligible. A mere 0.32 vol% addition of graphene to the polyacrylamide hydrogel led to an increment in the conductivity from 0.006 S m^{-1} to 1.8 S m^{-1}. It was also observed that the specific conductivity had a linear correlation with the amount of graphene added in the hydrogel. Hence, the conductivity of the hydrogel can be controlled through the adjustment of dopant concentration[66] as well as the choice of dopant.[67] One crucial point to consider for this group is the uniform distribution of the filler/dopant to ensure homogeneous conductivity throughout the hydrogel.

Hence, inherently conductive materials would seem as a more preferred option and there are many choices depending on the mechanism of the conductivity. Conductive polymers rely on the free electrons and holes whereas zwitterionic polymers utilize ions as the carrier to attain conductivity. In the conductive polymer category, numerous choices are available which include but not limited to polyaniline, polypyrrole, and poly(3,4-ethylenedioxythiophene). It was discovered that polymer conductive hydrogel could be attained simply by manipulating the environmental conditions without the need for crosslinkers. For instance, Losic *et al.* demonstrated that conductive polymer hydrogels could be formed by self-crosslinking of monomers or self-assembly based on supramolecular interaction without the use of additives.[68] The acquired polyaniline nanofiber hydrogels indicated a gravimetric capacitance of up to 492 F/g at an applied current density of 1 A/g.[68] In another study, Zhang *et al.* successfully achieved self-crosslinked conductive hydrogels with only oxidizing agent and precursor.[69] The derived polyaniline hydrogels electrodes realized a maximum capacitance of

294 approximately 750 F/g at an applied current density of 1 A/g.[69] Alternatively, zwitterionic
295 polymers could be introduced to equip hydrogels with the conductive function. This type of
296 polymers contains equal number of cations and anions on the molecular chains, which
297 essentially make the polymers neutrally charged. Under current flow, these free ions are
298 responsible for the conductivity. The main differentiating factor between the aforementioned
299 polymer types is the conductivity realized under direct and alternating current as the ions
300 present in the latter group could respond differently to the applied current type.
301 Methacryloyloxyethyl phosphorylcholine, [2-(methacryloyloxy) ethyl] dimethyl-(3-
302 sulfopropyl) ammonium hydroxide, carboxybetaine methacrylate, methyl methacrylate block
303 copolymer, and 2-(dimethylamino)ethyl methacrylate are some examples of zwitterionic
304 monomers.

305 Introduction of free ions to the hydrogels is another possible channel to tap on to enhance the
306 conductivity. It could be realized through the use of salt, acid, and/or alkali. The feasibility of
307 this strategy was demonstrated by Wu *et al.* in their recent study on the development of
308 hydrogel-based nitrogen dioxide sensor.[70] Infiltration of calcium chloride solution, more
309 specifically the chloride ions, was reported to bring about improved conductivity leading to
310 excellent sensitivity and low theoretical limit of detection. Additionally, they showed that the
311 use of higher concentration of calcium chloride solution (>1 M) enabled hydrogel to retain the
312 electrical properties even after 28 hours as compared to the loss of electrical conductance
313 within 5 h for pristine hydrogel and hydrogel exposed to 1 M calcium chloride solution. Similar
314 results were attained in another independent study conducted by Wu *et al.*.[71] Among the
315 various tested concentrations (10 wt%, 30 wt%, and 50 wt%), the highest concentration of
316 lithium bromide solution was identified to equip the hydrogel with the best conductivity (12 S
317 m^{-1}) which was a 30-fold increment. Apart from salt, acid and alkali are alternative sources of
318 free ions that could be imparted to the hydrogels for conductivity enhancement. For example,

319 the introduction of phytic acid to the poly(vinyl alcohol) hydrogel contributed free hydrogen
320 ions that led to the attainment of excellent conductivity (1.34 kΩ cm).[72] Double network
321 hydrogel based on poly(2-acrylamido-2-methylpropanesulfonic acid) and methyl cellulose
322 achieved a conductivity of 105 mS cm^{-1} at room temperature after concentrated potassium
323 hydroxide treatment.[73]

324 A second network targeting the conductivity part could be incorporated into the hydrogel
325 instead of fillers, dopants, and free ions. This technique is known as the double network system.
326 Fundamentally, the system consists of two individual networks with one delivering the
327 supporting function and the other targeting the conductivity part. The first network is usually
328 formed prior to soaking the gel in the precursor solution of the second network, which would
329 undergo *in situ* polymerization.[74] This method is appealing as the conductivity could be tuned
330 easily through adjusting the amount of second network present in the gel. While this design is
331 attractive with mild preparation method, it also comes with a complication. The hydrogel
332 matrix is hydrophilic in nature whereas most of the conductive polymers are hydrophobic.
333 Hence, the uptake of conductive polymers is inevitably affected resulting in uneven distribution
334 of the polymers and consequentially, inconsistent electrochemical properties throughout the
335 hydrogel. To promote uniform distribution of the polymers, Lu *et al.* improved the
336 hydrophilicity of polypyrrole through hybridization and doping with hydrophilic
337 polydopamine for better integration with the matrix.[75] The obtained hydrogel demonstrated
338 good conductivity (Figure 7). The success of double network technique provided inspiration to
339 Minev *et al.* to synthesize multi-network hydrogel.[76] Consequentially, a scaffold with high
340 similarity to the extracellular matrix was developed exhibiting good stretchability, tissue like
341 elastic modulus, and electrical conductivity of approximately 26 S m^{-1}.

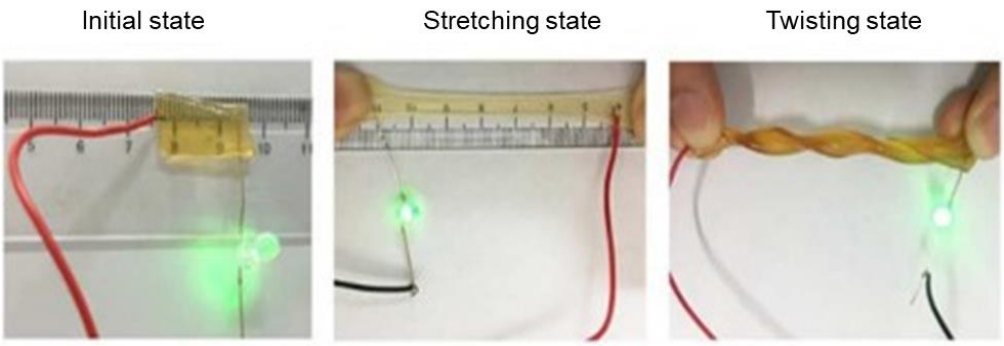

Figure 7. Images illustrating the conductivity of hydrogel based on polydopamine (PDA)-doped PPy nanofibrils. Reproduced with permission from ACS Publications.[75] Copyright 2018.

To further enhance the conductivity of the hydrogel, the aforementioned approaches could be employed together. For instance, Zhang *et al.* utilized polypyrrole (PPy) and trypan blue (TB) as the inherently conductive material and the dopants to form the conductive hydrogel.[67] The TB-doped PPy demonstrated improved electrically conductivity (3.3 S cm^{-1}) as compared to the PPy synthesized without TB.[67] Chen *et al.* also included both strategies in the construction of electrically conductive hydrogel.[77] Polyaniline, an inherently conductive polymer, was employed together with phytic acid, which was introduced into the gel as dopants to promote ionic interaction between polyaniline and phytic acid.

3.2. Mechanical Reinforcement

While the high-water content in the hydrogels gives them high similarity to extracellular matrices and makes them desirable for tissue engineering, the same feature (high-water content) is also the cause for their weak mechanical properties. With the flexibility of varying the crosslinking density and the choice of monomers, plenty of research efforts are invested in resolving the mechanical weakness of the hydrogel. Some of the explored methods include but not limited to the addition of fillers/dopants, the adoption of an effective energy dissipation

362 platform, the use of anisotropic material, the exploitation of microphase separation, and the
363 practice of hybrid system.

364 Addition of fillers/dopants is a common technique used to boost the mechanical properties of
365 the hydrogel. For example, calcium carbonate was introduced as a dopant to modify the
366 mechanical properties of the acetate chitosan hydrogel and the storage modulus improved by
367 approximately 60.88 Pa.[78] In theory, the enhanced mechanical properties of the gel could be
368 attributed to the electrostatic interactions between the amino group of the acetate chitosan and
369 the calcium ions of the dopant. In another study, nano-fibrillated cellulose functioning as the
370 filler and the dispersing agent was shown capable of improving the mechanical properties of
371 the hydrogels substantially.[79] The addition of nano-fibrillated cellulose into the
372 polyacrylamide-iron (II,III) oxide hydrogel increased the crosslinking density of the gel via
373 hydrogen bonding. Consequentially, the tensile strength and the elongation at break of the gel
374 improved by 630 chap and 1560% respectively.

375 In a system which exploits energy dissipation strategy, physical crosslinkers are utilized to
376 improve the mechanical properties of the hydrogel. The supramolecular system comprised of
377 Pluronic F127, AZO group, and β-cyclodextrin that served as amphiphilic copolymer, guest
378 groups, and host groups respectively.[80] The attained hydrogel achieved a fracture toughness
379 of 2.68 ± 0.69 MJ m^{-3} and a tensile strength of up to 475 kPa which were attributed to the
380 presence of both nano- and microscale energy dissipating structures in the form of reversible
381 switches and hydrophobic association in micelles.

382 Double network system, another notable method that emphasizes on the effective energy
383 dissipation, incorporates a second network into a pre-existing one to improve the mechanical
384 properties of the hydrogel. The earliest report of such systems could be dated back to 2004, in
385 which the two networks were made of bacterial cellulose and gelatin.[81] The concept behind

this strategy is to select one soft ductile network and one brittle network. Upon applied force, the brittle gelatin network would break to support the ductile bacterial cellulose network. A comparison among the elastic moduli obtained indicated that the double network hydrogels tested in the direction perpendicular to the stratified structure (1.7 MPa) was much better than the bacterial cellulose gel (0.007 MPa) and the gelatin gel (0.16 MPa). The synthesis of this hydrogel involved forming the first network prior to immersing the gel in the precursor of the second network followed by submerging in the crosslinker solution to form the second network. This technique was subsequently improvised with the ionic network being introduced as the second network. In this improved version, the ionic network consists of alginic acid and calcium chloride could unzip upon applied force, reducing the stress concentration experienced by the polyacrylamide network.[82] As such, the rest of network could remain intact during stress application. The synergy experienced by the hydrogel brought about by crack bridging and background hysteresis mechanisms was visible in the mechanical tests. The stress at rupture experienced by hybrid gel, alginate gel, and polyacrylamide gel were 156 kPa, 3.7 kPa, and 11 kPa, respectively. The stretch at rupture achieved by hybrid gel was 23 which exceeded alginate gel and polyacrylamide gel by 21.8 and 16.4 respectively. In another study, hydrogen bonding was identified as an important contributor for the high toughness possessed by the hybrid hydrogel. The work partially replaced polyacrylamide with polydimethylacrylamide while keeping the ionic network as alginic acid and calcium chloride.[83] It was discovered that modulus and toughness varied directly with the hydrogen bonding present, which in turn depended on the amount of polyacrylamide in the system. An increase in the hydrogen bonding through the use of poly (ethylene glycol) methyl ether methacrylate, within the range of 0-25 wt% in the system, achieved modulus and toughness between 200-600 kPa and 40-80 J m^{-3} respectively.

Another popular method to boost the mechanical properties of the hydrogel is through the

implementation of anisotropic structures. In the study conducted by Lu *et al.*, anisotropic structures were developed through aligning β-sheet-rich silk nanofibers in the direction of the electrical field while leaving amorphous silk nanofibers randomly aligned (Figure 8).[84] The derived hydrogel could withstand a compressive stress of 120 kPa which was much higher than the limit of 6.8 kPa set by amorphous silk nanofibers when tested in the orthogonal direction to the oriental nanofibers.

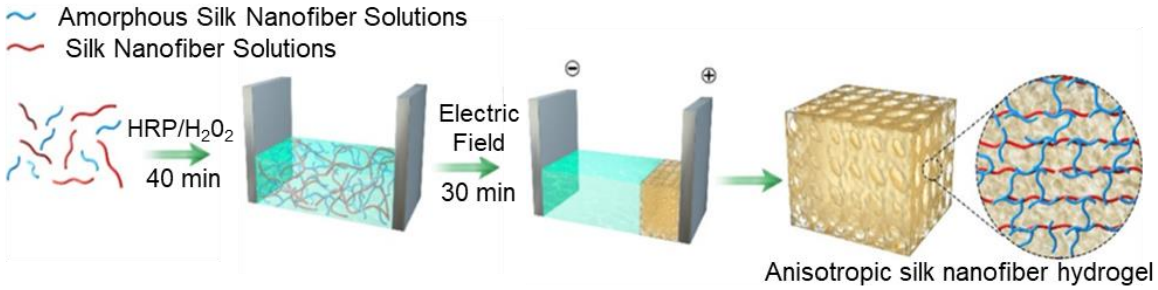

Figure 8. Schematic illustration of the synthesis process to obtain anisotropic tough silk nanofiber hydrogels. Reproduced with permission from ACS Publications.[84] Copyright 2020.

Microphase separation could be introduced to enhance the mechanical properties of the hydrogel. Thermal switching effect and Hofmeister effect are some explored means to achieve it. Adopting a similar approach exhibits by thermophiles proteins, Gong *et al.* designed poly(acrylic acid) hydrogels containing calcium acetate.[85] At elevated temperature, the developed hydrogels experienced dehydration which indirectly stabilized the ionic bonds between the components. As a result, area with polymer dense phase and polymer sparse phase was formed that participated in the reversible hardening of the hydrogels. This method had seen stiffness, strength, and toughness of the hydrogels improved by up to 1800-, 80-, and 20-folds respectively given a rise in temperature from 25 to 70 °C. In the latter technique, ammonium sulfate was widely examined as a kosmotrope to promote hydrophobic interaction and chain bundling within the polymer chains thereby leading to enhanced mechanical properties.[86] Wang *et al.* for instance reported that gelatin hydrogel after immersed in the

ammonium sulfate solution display an extraordinary ultimate strength of 12 MPa. In another separate work, poly(vinyl alcohol) hydrogel after immersed in the ammonium sulfate solution showed around 600 times increment in the elastic modulus.[87]

Several approaches described earlier could also be engaged simultaneously to bring about exceptional improvement to the mechanical properties of the hydrogel. This strategy was demonstrated very recently by Uyama *et al.*[88] They applied supramolecular guest-host interactions and reinforcing material concurrently to construct the hydrogel. The obtained hydrogel had a toughness of 38 ± 3 kJ m^{-3} which was likely due to the special design of using adamantine modified cellulose fibers as both the supramolecular crosslinker and the reinforcement element. Not only did the modified cellulose fibers boost toughness of the hydrogel by serving as crosslinkers, it also promoted the bonding between fillers and matrices via host-guest interactions that contributed to improved mechanical properties. Kim *et al.*, on the other hand, experimented with the use of double network system incorporated with inorganic filler and anisotropic element. Further improving on the existing alginate-polyacrylamide hydrogels system, mesoporous silica micro-rods were introduced as an inorganic filler and the double network was also remodeled to exhibit anisotropic hierarchical structure.[89] With the approach, they successfully obtained a swollen hydrogel that possessed tensile modulus of 7.2 MPa along with strength and toughness of 1.3 MPa and 1.4 MJ m^{-3} respectively.

Anisotropic structure had also been explored along with microphase separation as a potential way to build strong and tough hydrogels. He *et al.* prepared the anisotropic structure first by freezing-casting poly(vinyl alcohol) and the microphase separation was subsequently introduced by immersing the fabricated structure in sodium citrate solution.[90] The derived hydrogels successfully achieved ultimate stress, ultimate strain, and fracture energy of 23.5 ± 2.7 MPa, 2900 ± 450%, and 170 ± 8 kJ m^{-2} respectively.

458 *3.3. Self-Healing*

459 Self-healing ability is a desirable property especially for the development of wearable sensors.
460 With the ability to self-heal, the hydrogel could maintain the network integrity and potentially
461 other properties such as mechanical strength and elasticity, for long term usage. Various
462 methods have correspondingly been investigated for their relevance in realizing the self-healing
463 capability. They can be categorized under two major approaches, either based on dynamic
464 covalent bonds or noncovalent bonds.

465 One type of the dynamic covalent bonds that could be introduced to achieve self-healing
466 hydrogel is diol-borate ester bond. Yu *et al.* used polyvinyl alcohol and sodium tetraborate to
467 create diol-borate ester bonds in the hydrogel,[91] and they demonstrated these bonds were
468 capable of being cleaved and regenerated without any external stimulus. As a typical
469 demonstration, the hydrogel was divided into halves with the boundary marked by two different
470 colors. It was subsequently cut into halves according to the color boundary and left in physical
471 contact at room temperature. The two halves of the hydrogel merged and self-healed with no
472 gap detectable under the optical microscope (Figure 9). Imine and acylhydrazone bonds are the
473 other types of dynamic covalent bonds that could be incorporated into the network to attain
474 self-healing hydrogels. Chen *et al.* developed a hydrogel that contained these bonds through
475 the use of N-carboxyethyl chitosan, adipic acid dihydrazide and sodium alginate.[92] The
476 oscillatory shear strain tests with different strains and loading periods were performed on the
477 attained hydrogel to assess its recovery. It was revealed that the storage modulus restored
478 instantaneously after the applied strain was removed, independent of the loading period.

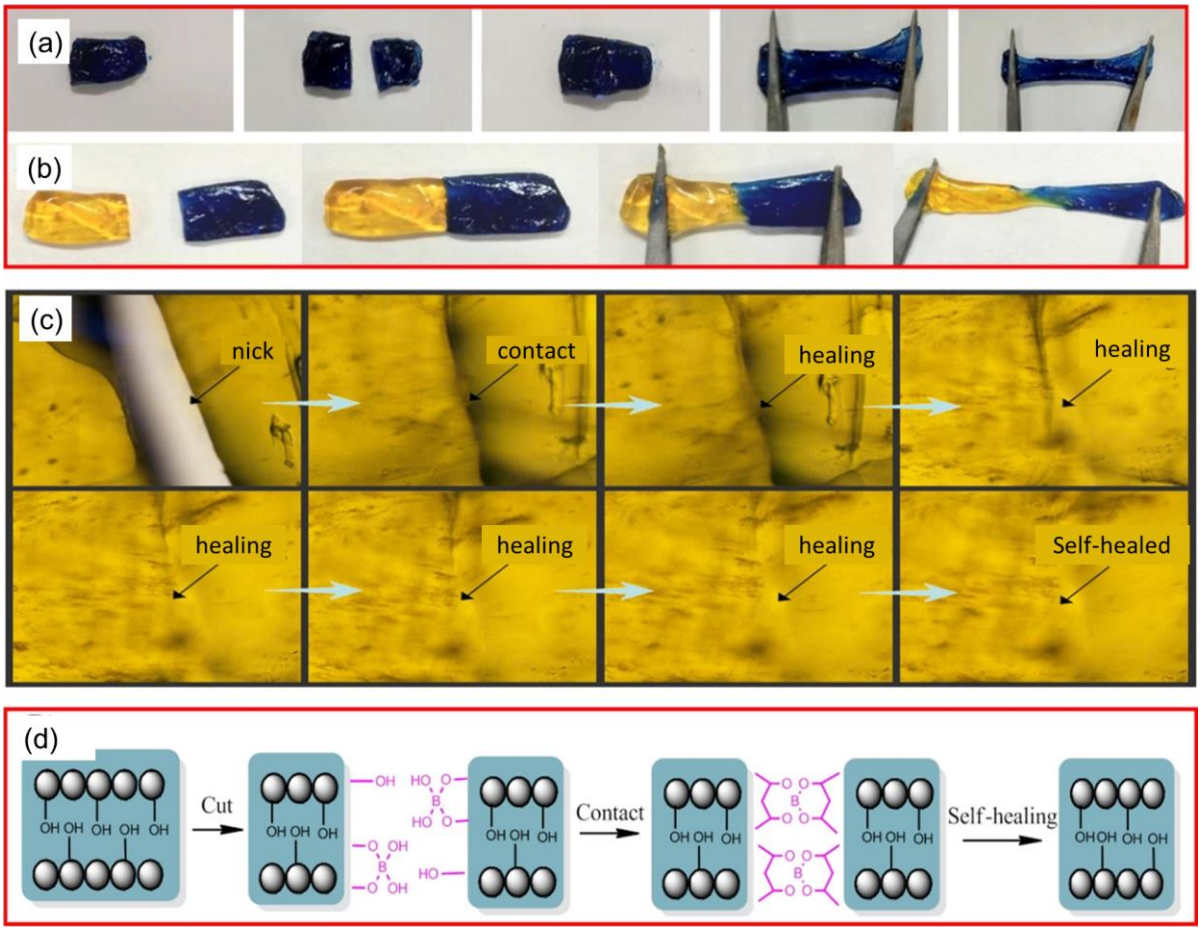

Figure 9. (a, b) Images demonstrating the self-healing properties of the hydrogels. (c) Optical microscopic images showing various stages of the self-healing process of the polyvinyl alcohol hydrogel. (d) Schematic illustrations of the self-healing mechanism. Reproduced with permission from Elsevier B.V..[91] Copyright 2019.

Dynamic noncovalent interactions, such as hydrogen bond and electrostatic complexation, could also be considered for the synthesis of self-healing hydrogels. As validated by Loh *et al.*, hydrogen bond was introduced through the interaction between acrylamide segments and chitosan backbone whereas inter-chain electrostatic complexation was incorporated via acrylic acid and chitosan.[93] They successfully demonstrated that four hydrogels, from different batches formed under the same conditions and compositions, could merge together in an hour after the hydrogels were placed in contact with each other. In addition, the hydrogel was found capable of recovering instantly followed the removal of applied strain greater than 12%. This

system also suggests that the existence of different types of bonds within a single hydrogel could potentially brought about synergistic effects. Therefore, the attained hydrogels could achieve repeated recovery in its mechanical properties.

In real life applications especially for the development of wearable sensors, multiple approaches have to be employed simultaneously. For example, Wang *et al.* designed a stretchable, adhesive, and self-repairing conductive structure color film for double-signal flexible electronic devices by introducing conductive carbon nanotube polydopamine packing into elastic polyurethane reverse opal scaffold.[94] The obtained film had stable tensile property and bright color structure. The film can be used for real-time color display because of its interactive color change during tensile process. Kim *et al.* reported a hydrogel with self-healing strain response electrochromic display. The hydrogel made from N, N '-methylenebisacrylamide can achieve 2000% tensile deformation. In addition, the circuit can visually display the bending of the finger.[95] Cui *et al*. created an interesting type of hydrogel with graphene oxide (GO), laponite clay and, hydrophobically associating polyacrylamide (HAPAM) infused into the gel matrix to enhance the mechanical properties of the hydrogel.[96] The GO/Clay/HAPAM hydrogel (GCHA) was physically crosslinked through hydrophobically associating domains and the nano-sheets of GO and laponite. The hydrogel was able to exhibit some useful properties such as high strength, conductivity, self-healing, and shape-memory abilities which are useful in applications such as biosensors for detection of body motion and dye separators for waste water treatment.

The integration of technology with biological systems require both biocompatibility and mechanical flexibility in the selected materials. Soft conductive materials are able to conform to irregular biological interfaces, improving contact with the native tissues for optimal efficacy. Through a combination of the aforementioned strategies, a tailored balance of the hydrogels'

517 mechanical, conductivity, and self-healing properties can realize revolution in the field of
518 electronic wearables.

4. Applications of Hydrogel-Based Flexible Electronics

The extremely high water content gives hydrogels physical similarity to native tissues, excellent biocompatibility, and the ability to encapsulate biomolecules/drugs.[13] It is well known that hydrogels are one of the common soft materials, and great efforts have been made to explore the potential applications of polymer hydrogels in flexible electronic devices.[97] Hydrogels with great mechanical toughness and elasticity have evolved to provide a versatile platform for integrating a variety of micro-devices such as retrievable circuit sensors, actuator transistors, and micro-ultracapacitors without the need for additional supporting substrates.[98]

4.1. Sensors

Sensors are devices/machines designed to mimic the intrinsic functions of human sensory organs that detect and respond to external signals.[24,99] The key function of a sensor is to convert physical or/and chemical stimuli into another form of energy.[99] Considering the long-term contact of such sensors with human skin or tissues,[100] they should be highly biocompatible, non-toxic, highly soft and flexible to meet the ergonomic, and safety requirements.[101] Hydrogels used in sensors are mainly for detection of human body signals. Hydrogel-based wearable sensors are believed to play an important role in medical diagnosis, biological signals detection, and other biologically relevant aspects. In order for hydrogels to function as sensors, hydrogels have to be responsive to external stimuli to generate feedback signals. Compared with traditional sensors, hydrogel sensors rely more on the unique properties of hydrogels, such as high water content, stimulation responsiveness, high permeability, etc.[24] Depending on the requirements, different hydrogels can be adopted to respond to different stimuli such as temperature, strain, etc. One simple way to achieve stimuli responsive hydrogels is through the addition of fillers (Table 1). At present, hydrogel-based biosensors have been applied in many fields, such as disease detection, environmental monitoring, field monitoring, etc.[102-104]

544 *4.1.1. Temperature Sensors*

545 Hydrogel-based temperature sensors generally convert the temperature stimulus into a
546 measurable physical response, being it geometric (Figure 10a),[105] optical (Figure 10b),[106,107]
547 or electrical (Figure 10c-i).[24,108,109] As the conductivity of hydrogels is proportional to the ion
548 mobility of hydrogels, their resistance is sensitive to the environmental temperature and thus
549 can be utilized to construct temperature sensors. For example, Lei *et al.* fabricated a type of
550 resistive temperature sensor by using polyzwitterionic poly (ammonium 3-
551 dimethyl(methacryloyloxyethyl)propanesulfonate) (PDMAPS), ion-rich 1-ethyl-3-
552 methylimidazolyl ethyl sulfate (IL), and hydrogen-bond donor poly (acrylic acid) (PAA) to
553 form a dynamic hydrogen-bonding networks.[108] This design ameliorated the shortcomings of
554 previous electronically conductive materials that are susceptible to large deformations,
555 maintaining >95% resistivity stability under 1000% deformation. At the same time, a high
556 transmittance of >90% and a super tensile strain of >10,000% were achieved due to the
557 presence of hydrogen bonds (Figure 10c-ii). Such excellent mechanical properties are rarely
558 mentioned in traditional conductive materials. Interestingly, Yu *et al.* synthesized a
559 polyethylene glycol hydrogel modified with gold nano-rods (AuNR) and Rhodamine B-
560 embedded silica nanoparticles (RhB@SiO_2).[107] This composite hydrogel was able to locally
561 induce a 3D temperature gradient by using the localized surface plasmon resonance (LSPR) of
562 AuNR under near-infrared laser irradiation. The local temperature change was instantaneously
563 probed by the fluorescence change of RhB@SiO_2 NPs due to the temperature-sensitive
564 fluorescence properties of Rhodamine B. A high-resolution of 0.74% $°C^{-1}$ was achieved for
565 temperature detection thanks to the synergistic effects of AuNR and RhB@SiO_2 encapsulated
566 in hydrogels (Figure 10d).

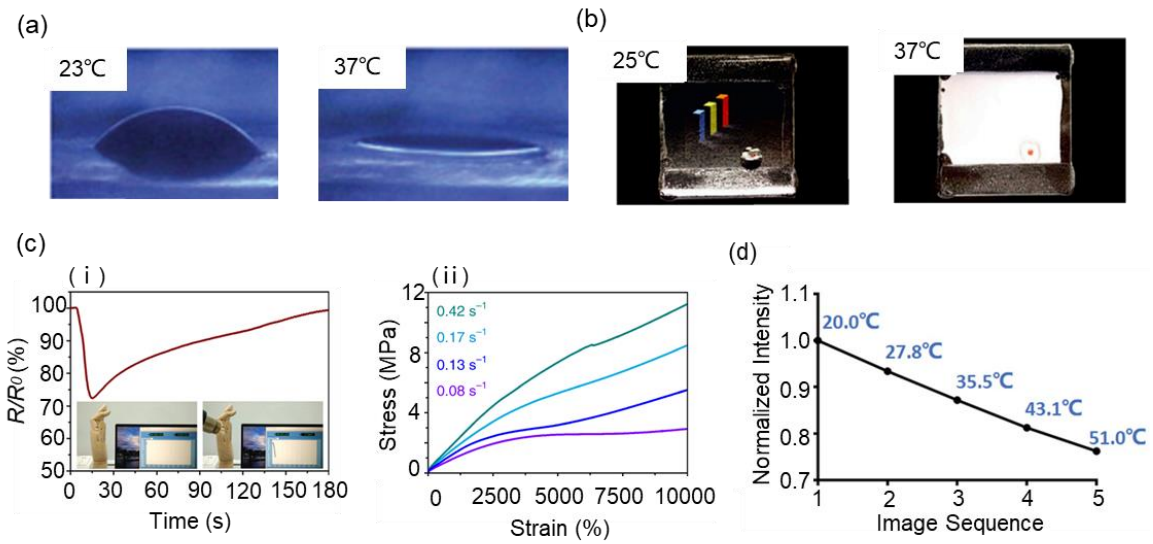

Figure 10. (a) Temperature-sensitive hydrogels with geometrical response. Reproduced with permission from Nature Publications.[105] Copyright 2006. (b) Temperature-sensitive hydrogels with optical response. Reproduced with permission from Elsevier B.V..[106] Copyright 2018. (c) (i) The sensor detects environmental temperature changes caused via resistance signals. (ii) The conductive hydrogel exhibits an ultra-long tensile strain of 10,000%. Reproduced with permission from Nature Publications.[108] Copyright 2019. (d) The fluorescence intensity of RhB@SiO_2 particles has a linear relationship with room temperature in the temperature range. Reproduced with permission from Wiley Publications.[110] Copyright 2021.

4.1.2. Chemical Sensors

Hydrogel-based chemical sensors generally convert chemical stimuli into changes in geometry[109,111,112] and optics[113] (Figure 11). Geometric changes of hydrogels are mainly resulted from volume changes of the polymer networks (swelling or shrinking) in solution. For example, Khademhosseini *et al.* invented an inexpensive and convenient method to incorporate mesoporous particles loaded with fluorescent dyes into alginate hydrogel fibers using a microfluidic spinning system, which was used to monitor the pH of the skin based on color changes (Figure 11a).[113] The pH response range of the hydrogel is 6.5-9. The pH sensing results can be directly captured by a smartphone camera and processed with the internal

MATLAB code. Since the pH of the wound reflects the healing of the wound to a certain extent, the system can monitor the pH in real-time and preliminarily assess the wound healing. In another study, Xu *et al.* designed a PEDOT:PSS conductive hydrogel as an electrochemical sensor for the detection of uric acid in sweat.[114] The detection of uric acid is mainly achieved by antibody-antigen-enzyme and chromogenic substrate. As the concentration of human uric acid is directly proportional to the optical density measured at 450 nm, the concentration of uric acid can be estimated. The sensor was designed based on this conductive hydrogel that exhibited a high sensitivity of 0.875 μA μM^{-1} cm^{-2} with a detection limit of 1.2 μM (S/N = 3) (Figure 11b). Lee *et al.* developed a muscle-inspired MXene PAA/PVA hydrogel as a pH and strain sensor for human muscle fatigue detection.[115] Since the pH of human sweat can reflect the fatigue degree of human muscles to a certain extent, the hydrogel sensor was used to gauge the muscle fatigue through targeting the sweat pH (Figure 11c-i). Specifically, the sweat pH variation was detectable by the change in the electrical resistance of the MXene negative charged surface. According to the pH of the environment, the cation selectivity of the MXene surface may become stronger or weaker. The detection of pH between 3-6 was achieved (Figure 11c-ii).

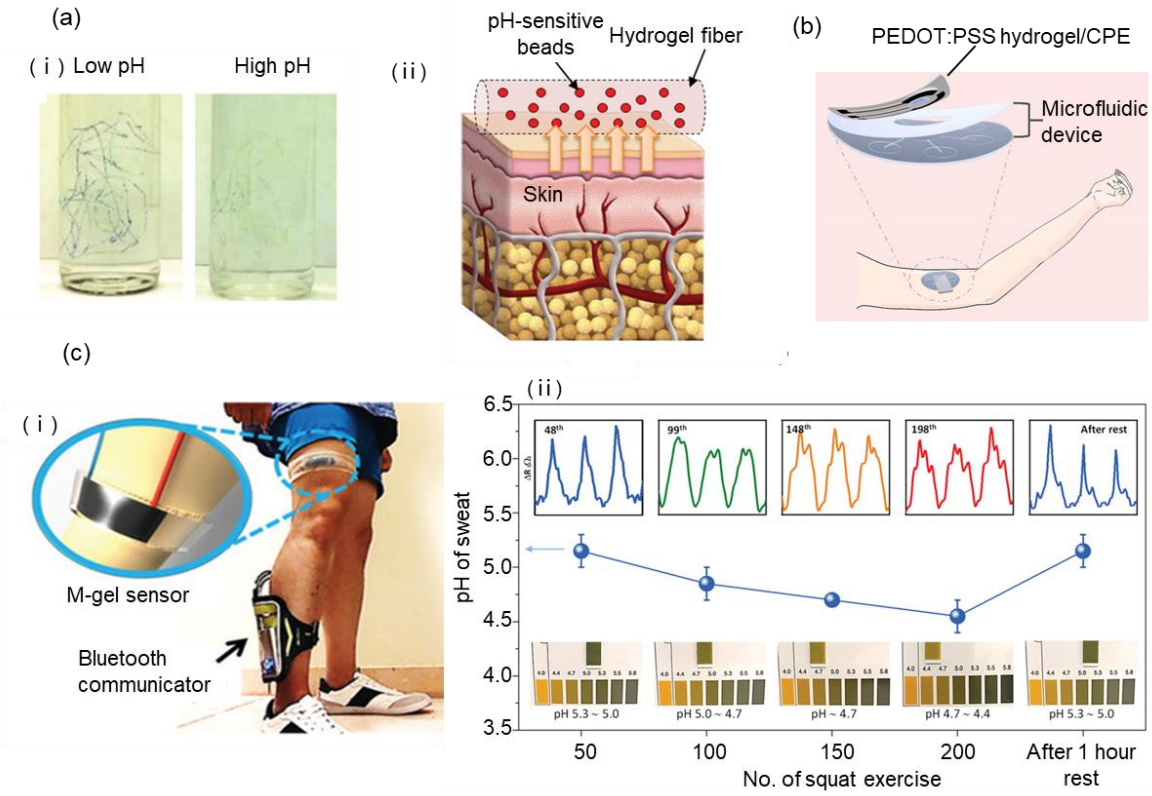

602

603 **Figure 11.** (a) (i) An image of pH responsive bead-laden hydrogel microfibers. (ii) A schematic
604 illustration of the pH-sensing hydrogel microfibers designed for long-term epidermal
605 monitoring. Reproduced with permission from Wiley Publications.[113] Copyright 2016. (b)
606 Schematic representation of the wearable uric acid sensor. Reproduced with permission from
607 Elsevier B.V..[114] Copyright 2021. (c) (i) Wireless sensory hydrogel sensor to detect muscle
608 fatigue by detecting pH. (ii) Corresponding resistance changes measured over different number
609 of movements (upper insets). Changes in pH under different exercise number of movements
610 (lower insets). Reproduced with permission from Wiley Publications.[115] Copyright 2021.

611

612 *4.1.3. Stress/Strain Sensors*

613 The stress/strain sensor is generally formed by sandwiching a dielectric between two layers of
614 hydrogel as a capacitive hydrogel stress/strain sensor. The change in the distance between the
615 two hydrogel layers is mainly caused by an external force, and altering the contact area between
616 the hydrogel and the dielectric, will lead to a change in the capacitance. By measuring the
617 capacitance, the stress/strain can be gauged.[116-119] Suo *et al.* proposed the concept of "ionic

skin" for the first time and developed an electronic skin that can be used as a strain/stress sensor (Figure 12a-i).[116] The electronic skin was constructed by sandwiching two NaCl-containing polyacrylamide hydrogels (as the ionic conductor) with an acrylic elastomer (as the dielectric medium). The ionic skin sensor not only easily resolved the pressure of gentle touch by fingers (< 10 kPa) (Figure 12a-ii), but also detected the location of pressing (Figure 12a-iii). Zhang *et al.* prepared an all-flexible self-powered integrated system, which was composed of MXene hydrogel as a pressure sensor in series with solar cells and lithium-ion micro-batteries (Figure 12b-i).[120] Excitingly, the system was very sensitive to body movements, with a response time of 35 ms. A highly integrated packs of 100 MXene-based micro-supercapacitors in series can give the highest voltage output for MXene-based micro-supercapacitor to date, 60 V (Figure 12b-ii). Shen *et al.* used a capacitive pressure sensor to prepare a robot prosthesis with tactile sensing.[121] This pressure sensor was fabricated with PAAm-NaCl hydrogel and conductive fabrics through a facile fabrication method (Figure 12c-i). The pressure sensor exhibited a high sensitivity of 1.5 kPa^{-1} due to its ultra-high capacitance per unit area of about 2.14 μF cm^{-2} (Figure 12c-ii). And the response time of the sensor (18 ms) was significantly shorter than that of human skin (40 ms). The sensor opens up new possibilities for next-generation intelligent robotic systems. Guo's group has developed many stimuli-responsive hydrogels. For example, they made the hydrogels conduct electricity by introducing conductive substances into PNIPAM, which can be used to detect joint bending signals and have good biocompatibility [122,123]

On the other hand, due to the stretching of hydrogel by external force, if the length of hydrogel increases by *a* times and the width decreases by *a* times, the resistance of hydrogel becomes a^2 times as before.[118,124-126] Based on the relationship between mechanical deformation of hydrogel and resistance, a hydrogel resistance strain sensor is established. According to the change detected in hydrogel resistance, the corresponding mechanical deformation can be

643 calculated. Zheng *et al.* developed a new type of zwitterionic hydrogel.[127] The hydrogel was
644 made with 3-(1-(4-vinylbenzyl)-1H-imidazol-3-ium-3-yl) propane-1sulfonate as the monomer.
645 Interestingly, the hydrogel can not only be used as a strain sensor, but also has a fracture
646 elongation ratio of 4.5 and a fracture stress of 200 kPa (Figure 12d). The enhanced mechanical
647 properties of this hydrogel were mainly due to the enhanced chain stiffness, interchain
648 interactions, and associative strength of the polymer-rich phase after the introduction of
649 benzene and imidazole groups, as well as the microphase-separated structure. Compared with
650 the conventional zwitterionic hydrogel, this hydrogel showed an increase in stretchability and
651 fracture toughness by 40 times and 60 times, respectively. Cai *et al.* prepared an acrylonitrile
652 copolymer hydrogel that can be used as a strain sensor by relying on the structural
653 characteristics of plastic elastomer micro-phase separation and physical crosslinking.[126] The
654 derived hydrogel had good shape memory properties, and a shape stability that can be
655 maintained for at least 60 days under the condition of not affecting the strength of the hydrogel
656 in an aqueous environment (Figure 12e). The acrylonitrile hydrogel can be processed cyclically,
657 and the maximum fracture energy can reach up to 7,592 J m^{-2}. Besides the studies of single-
658 channel strain sensors, Lin *et al*. designed a dual-channel hydrogel flexible strain sensor.[128]
659 The sensor converted strain into electrical and optical signals (Figure 12f). The sensor consists
660 of an interface-bound fluorescent hydrogel, carbon nanotube film, and polydimethylsiloxane.
661 The tightly packed carbon nanotube films can precisely control the formation of stretch-
662 induced network micro-cracks, allowing the sensor to simultaneously output electrical and
663 optical signals.

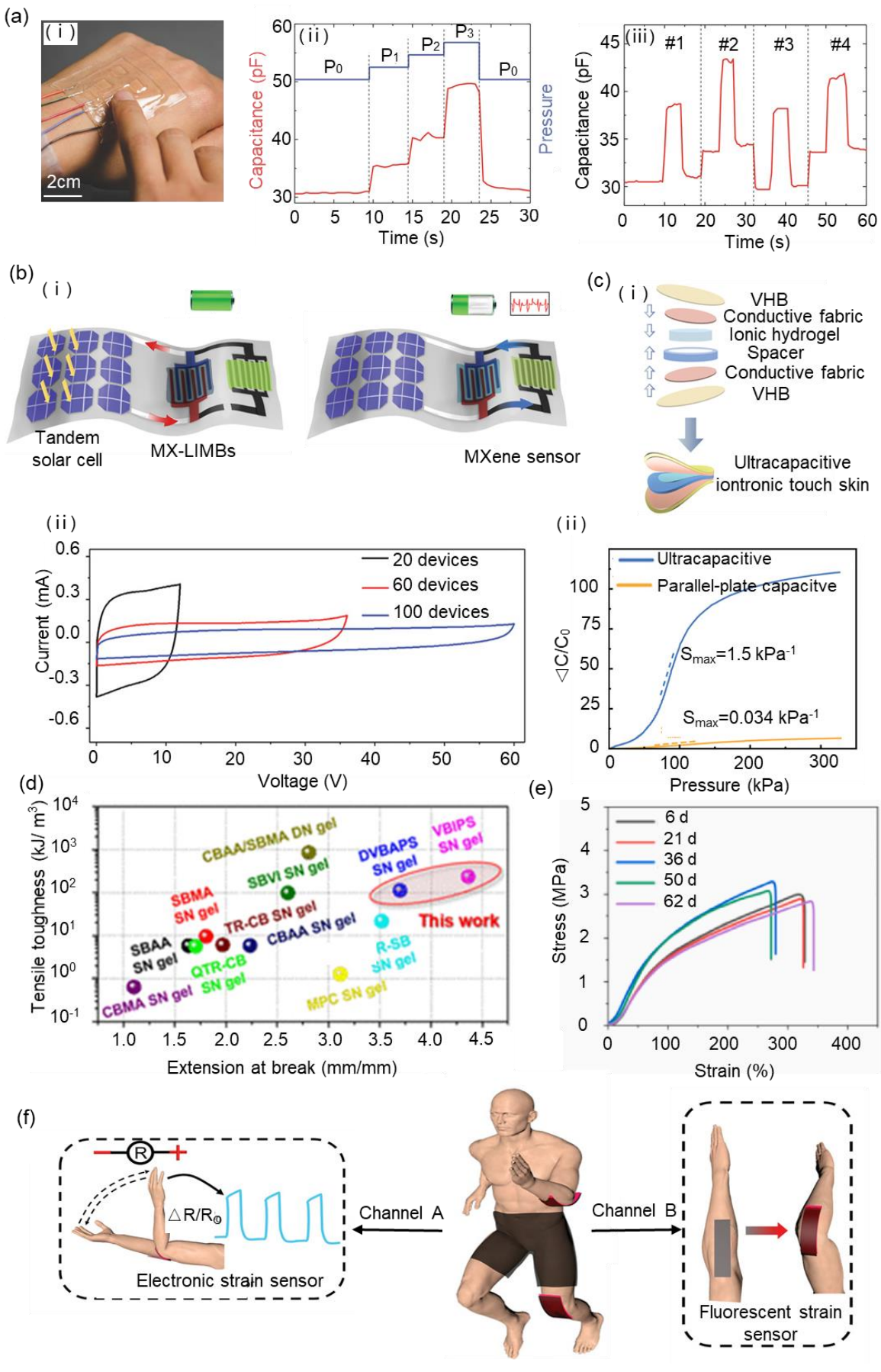
(a)
(i)
2cm
(ii)
P0
P1
P2
P3
Capacitance (pF)
Pressure
Time (s)
(iii)
#1
#2
#3
#4
Capacitance (pF)
Time (s)
(b)
(i)
Tandem solar cell
MX-LIMBs
MXene sensor
(c)
(i)
VHB
Conductive fabric
Ionic hydrogel
Spacer
Conductive fabric
VHB
Ultracapacitive iontronic touch skin
(ii)
20 devices
60 devices
100 devices
Current (mA)
Voltage (V)
(ii)
Ultracapacitive
Parallel-plate capacitve
Smax=1.5 kPa-1
Smax=0.034 kPa-1
ΔC/C0
Pressure (kPa)
(d)
CBAA/SBMA DN gel
SBVI SN gel
DVBAPS SN gel
VBIPS SN gel
SBMA SN gel
TR-CB SN gel
CBAA SN gel
This work
SBAA SN gel
QTR-CB SN gel
R-SB SN gel
CBMA SN gel
MPC SN gel
Tensile toughness (kJ/ m3)
Extension at break (mm/mm)
(e)
6 d
21 d
36 d
50 d
62 d
Stress (MPa)
Strain (%)
(f)
R
ΔR/R0
Electronic strain sensor
Channel A
Channel B
Fluorescent strain sensor

664

Figure 12. (a) (i) Pressure sensor attached to the back of the hand. (ii) This sensor detected the pressure of the touch. (iii) The sensor detected the location of the touch. Reproduced with permission from Wiley Publications.[116] Copyright 2014. (b) (i) Schematic illustration of charging and sensing of an all-flexible self-powered integrated pressure sensing system based on MXene. (ii) CV curves of 20, 60, and 100 tandem MXene-based micro-supercapacitor. Reproduced with permission from Wiley Publications.[128] Copyright 2021. (c) (i) Diagram of a pressure sensor used as ultra-capacitive iontronic touch skin. (ii) Comparison of pressure sensitivity between this ultra-capacitive iontronic pressure sensor and traditional parallel plate capacitive sensor. Reproduced with permission from Wiley Publications.[121] Copyright 2021. (d) Diagram of the mechanical properties of the pure zwitterionic hydrogels. Reproduced with permission from ACS Publications.[127] Copyright 2021. (e) Tensile stress-strain curves of the P(AN/AANa)-15 hydrogels with different swelling time. Reproduced with permission from Elsevier B.V..[126] Copyright 2021. (f) Scheme showing two-way electronic and fluorescent color responses to human motion. Reproduced with permission from Wiley Publications.[129] Copyright 2021.

4.1.4. Humidity sensors

Humidity sensing is used in many fields, such as food, biology, textile, and so on.[99,130] Humidity detection mainly depends on the change in resistance or color.[131,132] As the polymer network structure of hydrogel contains a large amount of water, a certain amount of ions can be dissolved in the hydrogel to form ionic hydrogel. The resistance of ionic hydrogel is determined by the carrier concentration and ions mobility in the ionic hydrogel. The change in relative humidity leads to the change in water amount present in the hydrogel and consequently, a change of ion concentration in the ionic hydrogel. Given that the ion migration in hydrogels is affected by the change of ion concentration (Figure 13a), the change in humidity can be identified through the current change.[131] Gao *et al.* developed a hydrogel thin film humidity and temperature sensor with a thickness of only 0.1 mm.[133] The hydrogel sensor can detect 20%-90% relative humidity and -30-50 °C temperature. The response time and recovery time were only 0.41 s and 0.3 s. Chitosan-gelatin-glycerin-NaCl (CGGN) was the main component

of the hydrogel (Figure 13b). In another work, Yu *et al.* prepared highly conductive hydrogels by solvent replacement of cellulose nanofibers (CNFs) and $CaCl_2$/sorbitol solutions.[134] Due to the addition of $CaCl_2$/sorbitol, the hydrogel had a temperature resistance of -50 °C, a water retention rate of over 90%, and a relative humidity detection range of 23%-97%. A possible explanation for the enhanced mechanical properties observed can be attributed to the formation of dynamic linking bridges and front layered honeycomb-like structure in the hydrogel, brought about by the addition of CNFs. As CNF is a bio-derived material, this humidity sensor is likely to be biocompatible for use in the human body.

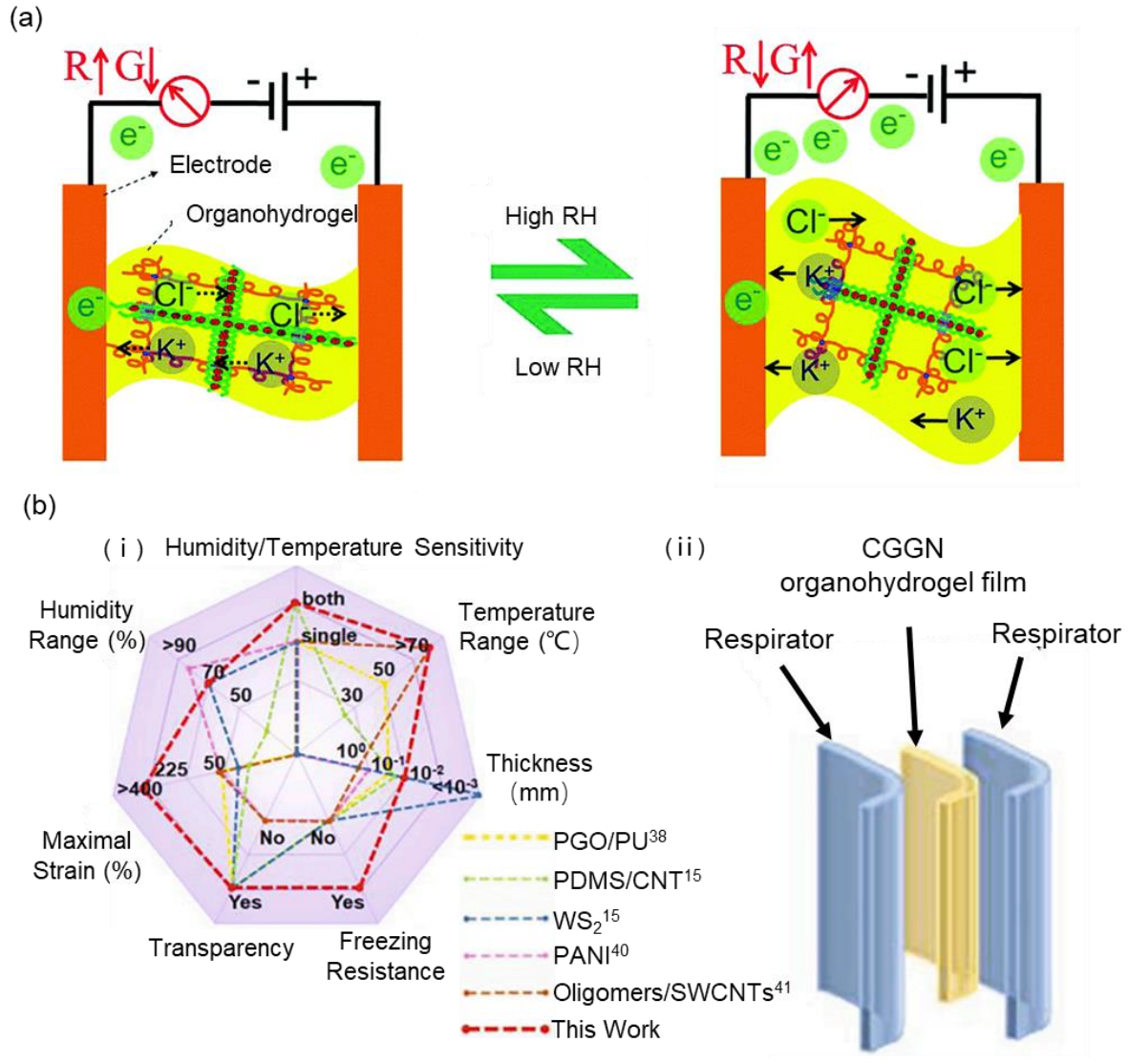

Figure 13. (a) Schematic illustrating the humidity sensing principle of the hydrogel.

Reproduced with permission from RSC publications.[131] Copyright 2019. (b) (i) The hydrogel has good temperature and humidity sensing properties. (ii) Schematic diagram of the humidity response of the CGGN hydrogel sensor sandwiched between two layers of respirators. Reproduced with permission from Elsevier B.V..[133] Copyright 2022.

708 **Table 1.** Representative examples of hydrogel-based flexible electronics.

	Category	Hydrogel	Input	Output	Performance	Requirements	Reference
Sensors	Temperature sensors	PVA-DMSO	Temperature	Electrical response	Range of temperature (-30-60 ℃); high toughness (3.1 MPa, 600%).	Response to temperature stimuli or/and being conductive.	[135]
		N-phenylaminomethyl POSS	Temperature	Optical response	Its transmission being modulated automatically upon environmental temperature shifts; the high toughness and high stretchability (10000% strain).		[136]
		PDMAPS-IL-PAA	Temperature	Electrical response	Ultra-stretchable (>10000% strain); high- modulus (> 2 MPa Young's modulus); self-healing; highly transparent (> 90% transmittance).		[108]
	Chemical sensors	PAAm-PAAc	pH	Geometrical response	Designing a robust chemomechanical sorting system capable of the concerted catch and release of target biomolecules from a solution mixture.	Response to pH, antigens, or other chemicals, being conductive.	[111]
		Alginate-pH-responsive beads	pH	Optical response	Hydrogel microfibers containing mesoporous particles loaded with a pH-responsive dye developed.		[113]
		Antigen-antibody semi-IPN	Specific antigen	Geometrical response	A material swelling reversibly in a buffer solution in response to a specific antigen.		[112]
		PEDOT:PSS	Uric acid	Electrical response	Ultrahigh sensitivity of 0.875 μM^{-1} cm^{-2} and a low limit of detection down to 1.2 μM.		[114]
		Ionic polyacrylamide	Pressure	Electrical response	High sensitivity of 2.33 kPa^{-1} with a capacitance	Being conductive.	[137]

				sensitivity of 103.8 nF/kPa.		
	Strain/Stress sensors	PEA-r-PS-r-PDVB [EMI][TFSI]	Pressure	Electrical and optical dual response	High sensitivity of ~152.8 kPa^{-1}, a broad sensory pressure range (up to 400 kPa), and excellent durability (>6000 cycles).	[138]
		PAAm-NaCl	Pressure	Electrical response	Broad pressure detection range of over four orders of magnitudes (≈35 Pa to 330 kPa), ultrahigh baseline of capacitance, and fast response time (18 ms).	[139]
		PDA-clay-PSBMA	Strain	Electrical response	Sensitivity of 4.3; wireless transmission of signals captured by the hydrogel sensors.	[140]
	Humidity sensors	Poly-carboxybetaine	Humidity	Electrical response	Fast response (0.27 s), recovery time (0.3 s), and wide relative humidity detection range (4-90%).	Being sensitive to humidity and conductive.	[131]
		Gelatin, glycerol, chitosan, and sodium chloride	Humidity	Electrical response	The RH detection range of 20%-90% and the recovery time is only 0.41 s.		[133]
Energy harvest devices	TENG (Harvest of electricity)	PVA	Mechanical energy	Electric energy	The open-circuit voltage of TENG can reach up to 92% of the output voltage; recyclable.	Being conductive and excellent stretchability.	[141]
		Polyacrylamide/montmorillonite/carbon nanotube	Mechanical energy	Electric energy	Temperature toleration (-60 to 60 °C); ultra-wide strain range (0-4196%) with a high sensitivity of 8.5.		[142]
		PAM-HEC-LiCl	Mechanical energy	Electric energy	The TENG achieved an output of 285 V, 15.5 mA, 90 nC, and a peak power density of 626 mW m^{-2}.		[143]

		PAM	Mechanical energy	Electric energy	Using in anticorrosive and harsh environment.		[144]
	Harvest of ultrasound energy	$Ti_3C_2T_x$-PVA	Ultrasound energy	Electric energy	A device is designed to convert ultrasonic energy into electrical energy.	Ultrasonic absorbing, being conductive.	[145]
	Harvest of salinity gradient energy	PSS-agarose	Osmotic energy	Electric energy	Power densities of 5.06 W m^{-2}.	One-way flowing, being conductive.	[146]
Energy storage devices	Capacitor	Poly(acrylic acid)	\	\	High power density of 15.7 kW kg^{-1}; energy efficiency of 98%.	Being ionically conductive.	[147]
	Battery	Sodium poly-acrylate hydrogel (PANa)	\	\	High cycling stability; high capacities.		[148]
Actuators		Acrylic acid, 2-hydroxyethyl methacrylate, and ethylene glycol dimethacrylate	pH	Geometrical response	Autonomous control of local flow; short response time (< 10s).	Response to temperature, pH, light, magnetic field. etc.	[149]
		Acrylic acid, acrylamide	pH	Geometrical response	Dual pH response controls lipophilic drug release.		[13]

N-isopropylacrylamide, 4-hydroxybutyl acrylate, and graphene oxide	Light	Geometrical response	Fast response to NIR (187.7°/s).	[150]
Acrylamide, silver nanoparticles	Light & pH	Geometrical response	Significant anisotropy in optical and swelling/detumescence deformation.	[151]
Poly(acrylic acid-co-acrylamide), poly(N-isopropylacrylamide), and graphene oxide	Temperature & Light	Geometrical response	Dual control of NIR and temperature.	[152]
Acrylamide, poly(2acrylamido-2-methylpropanesulfonic acid), and triethylene glycol	Electricity	Geometrical response	The tensile stress at break increased from 0.114 MPa to 5.6 MPa, and the strain increased from 32% to 159%.	[153]
Acrylic acid, poly(ethylene glycol) diacrylate, and phenylbis(2,4,6-trimethylbenzoyl) phosphine oxide	Electricity	Geometrical response	Soft robotic manipulation and locomotion with 3D printed electroactive hydrogels.	[154]
Sodium alginate, Fe_3O_4 nanoparticles, 1-hydroxybenzotriazole, 1-	Magnetic field	Geometrical response	Large deformation and more than 70% volume change under moderate magnetic field.	[155]

	ethyl-3-(dimethylaminopropyl) carbodiimide, and adipic acid dihydrazide					
Transistors	Polyethylene glycol, penicillinase	Penicillin	Electrical response	Real-time, label-free detection of penicillin within 0.2 mM.	Being conductive, easy to mould and easy to package the detected material.	[156]
	Polyacrylamide	Pressure	Electrical response	High sensitivity of 2.33 kPa^{-1} with a capacitance sensitivity of 103.8 nF/kPa.		[137]
Electromagnetic shielding	MXene, poly(acrylic acid)	Electromagnetic waves	/	In a hydrogel with a thickness of 0.13 mm, a high EMI SE of 45.3 dB, and an effective absorption bandwidth of 0.2 ~ 2.0 THz with an excellent reflection loss of 23.2 dB can be obtained.	High water content, including electromagnetic shielding filler.	[157]
	CNF, MWCNTs, and polyacrylamide	Electromagnetic waves	/	EMI shielding efficiency (≈28.5 dB) is improved by 90%.		[158]
Touch screen	Polyacrylate, LiCl	/	Electrical response	A hydrogel ionic touch panel that can freely transmit optical information.	Being conductive and transparent.	[159]
	3-[dimethyl-[2-(2-methylprop-2-enoyloxy) ethyl] azaniumyl] propane-1-sulfonate, nanoclays	/	Electrical response	Self-healing, pressure-sensitive, transparent, and highly stretchable surface capacitive touchscreens.		[97]

Devices for Controlled Drug Release	Zwitterionic poly-carboxybetaine, phenol red, glucose oxidase, and horseradish peroxidase	pH & glucose	Optical response	Monitor pH in the range of 4-8 and glucose concentration in the range of 0.1-10 × 10^{-3} m.	Drug encapsulation and release, being stimuli-responsive, and biocompatibility.	[160]
	PNIPAM, alginate	Temperature & pH	Electrical response	A networked closed-loop automated patch monitoring and treatment of chronic trauma.		[161]
	Acrylate-PEG acrylate	UV	/	An intelligent flexible electronic integrated wound dressing; real-time monitoring of wound temperature; drug release on demand.		[54]

709

4.2. Energy harvest devices

With the increasing phenomenon of global warming, environmental and energy problems have attracted more and more attention.[162,163] Nowadays, fossil fuels are still the main source of energy for people's daily life. However, fossil fuels are not an inexhaustible source of energy, so we need to develop new energy harvesting devices to acquire previously inaccessible energy or to reduce energy consumption to ensure sustainable development for future generations. In addition, the use of fossil fuels can easily cause environmental problems.[162] The recent development of flexible electronic devices, such as electronic skin, soft robot, flexible medical monitoring equipment, and so on, has seen the emergence of flexible energy collection devices. The unique biocompatibility and high water content of hydrogels combine electronic devices and living organisms. Equipped with many unique properties, such as biocompatibility, high softness, elasticity, biodegradability, rapid diffusion, etc., hydrogel-based devices can collect all kinds of energy and then achieve the purpose of energy recovery.[143] In particular, some hydrogels have self-healing properties and good tensile properties, which endow energy harvesting devices with more deformable properties. Here, hydrogels are mainly used as electrodes, especially for triboelectric nanogenerators, and the hydrogels are required to have good electrical conductivity.

Triboelectric nanogenerators (TENG) convert mechanical stimuli to electrical energy through triboelectric and electrostatic induction, enabling the construction of self-powered sensors or systems.[10,164-166] The collected electrical energy was determined by the contact separation of the electrodes (Figure 14a).[142,167] The flexible and non-toxic properties of hydrogels can be imparted to hydrogel-based TENG making them one of excellent material choices for TENG. Xu *et al.* developed a hydrogel-based TENG (Figure 14b) that functioned as a self-powered sensor to detect human movement.[141] The hydrogel TENG used recyclable polyvinyl alcohol as raw material, which is more environmentally friendly. The TENG achieved a peak output

power of 2 mW when loaded with a resistance of 10 MΩ. Bao *et al.* synthesized an antifreeze hydrogel by one-step free radical polymerization of acrylamide monomer in hydroxyethyl cellulose aqueous solution, and then used lithium chloride (LiCl) to further improve the frost resistance of the hydrogel.[143] Due to the introduction of LiCl solute particles into the hydrogel, the decrease in vapor pressure lowered the freezing point of the solution. The hydrogel was employed as nanogenerator for harvesting biomechanical energy to drive wearable electronic devices, even in harsh cold ice and snow environments as low as -69 ℃ without freezing. The fabricated 3×3 cm^2 TENG achieved open-circuit voltage, short-circuit current, and transferred charge of 285 V, 15.5 mA, and 90 nC, respectively, at a frequency of 2.5 Hz. Wang *et al.* developed a chemically stable hydrogel for TENG electrodes.[144] The chemical stability of the hydrogel is mainly due to the unique sliding ring structure of the cross-linked PAM polymer and the long chain of cyclodextrin molecules (Figure 14c).

Ultrasonic power can be also utilized to generate energy. Lee *et al.* demonstrated that a MXene-PVA hydrogel implanted generator was capable of converting ultrasonic energy into electrical energy (Figure 14d) and an output voltage of 2.8 V was achieved.[145] Combined with frictional electrification, the output power of the generator can be increased.

The Gibbs free energy, otherwise known as the salinity gradient energy (SGE), can be gauged by comparing the salinity difference between the salt water and fresh water of the ocean.[120,162] Hence, the ocean is an untapped source that has the potential to be further explored for energy harvesting. By mixing polyelectrolyte hydrogel and aromatic polyamide nanofiber membrane, Zhang *et al.* realized high performance osmotic energy conversion (Figure 14e-i), and successfully converted salinity gradient into electric energy.[146] The high performance could be attributed to the charged three-dimensional network constructed from poly (sodium 4-styrenesulfonate), agarose, and various electrolytes that facilitated ion diffusion (Figure 14e-ii). Additionally, the ion diffusion was further improved with the introduction of an aramid

760 nanofiber membrane to the hydrogel that resulted in a high power density of 5.06 W m^{-2}. In
761 another work, Tan and coworkers developed a photoanode-hydrogel-solar cell series system
762 from mainly $CoCl_2$ and 2-methoxyethanol to harvest energy from the atmospheric water.[168]
763 The derived multifunctional hydrogel was capable of absorbing water from the air and the
764 photoanode modified by the $BaTiO_3$ @$BiVO_4$ hybrid material utilized the absorbed water to
765 generate electricity, thereby realizing energy conversion. A photocurrent of 0.4 mA cm^{-2} in
766 water was recorded under an illumination of 10 mW cm^{-2} (Figure 14f), providing new insights
767 into atmospheric water separation.

768 Various photon and energy conversion devices release a lot of heat during use, such as
769 computing microprocessors, light-emitting diodes (LEDs), and so on. Pu *et al.* designed an
770 intelligent thermoelectric flow gel with monomers $K_4Fe(CN)_6$ / $K_3Fe(CN)_6$, acrylamide, and
771 additives lithium bromide, to convert the low-grade waste heat generated by the devices into
772 electric energy.[169] Aside from energy recovery, the smart thermocouple hydrogel film
773 concurrently promoted heat dissipation which helped to protect the equipment and prolong its
774 lifespan. As a demonstration, a 2 mm thick hydrogel was attached to the battery of an electronic
775 device. It was observed that the battery temperature was reduced by 20 °C and 5 μW of
776 electrical energy was recovered by the hydrogel film at a discharge rate of 2.2 C.

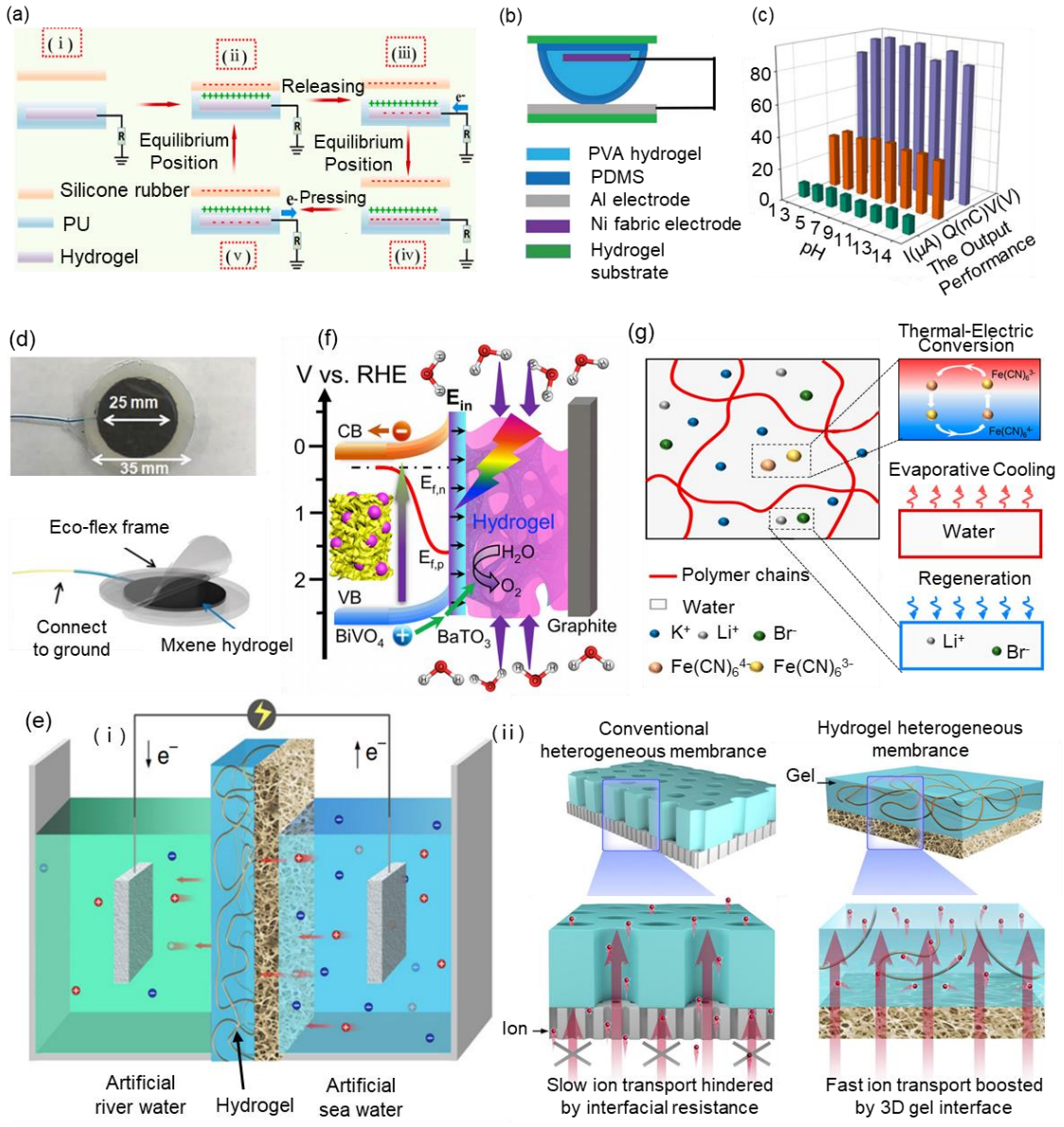

Figure 14. (a) Sandwich-structured STENG and schematic diagram to clarify the working principle of the STENG. Reproduced with permission from Elsevier B.V..[142] Copyright 2020. (b) Schematic of the standard hydrogel-based triboelectric generator. Reproduced with permission from Wiley Publications.[141] Copyright 2017. (c) The output performance of the circulating hydrogel electrodes at different pH was compared. Reproduced with permission from Elsevier B.V..[144] Copyright 2021. (d) Photo and schematic illustration of the MXene-PVA hydrogel generator. Reproduced with permission from RSC Publications.[145] Copyright 2020. (e) (i) Schematic of the osmotic energy conversion process. (ii) Three-dimensional hydrogel interface with high transport efficiency. Reproduced with permission from Nature Publications.[146] Copyright 2020. (f) Schematic of the photoanode-hydrogel-solar cell series system. Reproduced with permission from Elsevier B.V..[168] Copyright 2019. (g) Schematic of

working principle of the smart thermos-galvanic hydrogel. Reproduced with permission from ACS Publications.[169] Copyright 2021.

4.3. Energy storage devices

With the development of flexible wearable devices, the energy supply of flexible wearable electronic devices has attracted wide attention.[170] Electrochemical energy storage devices usually consist of two electrodes and an electrolyte between them.[171] The highly abundant and tunable chemistry of hydrogels allows the introduction of new functions into existing hydrogels, making it possible to create unprecedented energy storage devices with additional functions.[172] The charged functional groups on the polymer chain effectively attract and locate the electrolytic ions in the network, while large amounts of solvent water (up to 2,000 times its own weight) can be absorbed and trapped in the frame.[172,173] Since the hydrogel has the characteristics of high water content, this allows them to have ionic conductivity similar to liquids, while the dimensional stability of solids is maintained, which is ideal for flexible energy storage devices.[172,174]

Electrochemical capacitors, in principle, store charge by the adsorption/desorption of electrolyte ions on the electrode surface.[145] Huang *et al.* reported new electrolytes consisting of sodium polyacrylate hydrogel (PANa) with either Zn//NiCo or Zn-Air rechargeable batteries (Figure 15a).[148] Both types of electrolytes displayed ultra-long cycle stability (16000 cycles, capacity maintenance 65%, and 800 cycles for 160 h), each an order of magnitude higher than the best solid-state counterpart. Fu *et al.* developed an anti-freezing zinc-hybrid hydrogel capacitors with high electrical conductivity and great interfacial adhesion.[175] The monomers of this hydrogel are [2(methacryloyloxy)ethyl] dimethyl (3-sulfopropyl) and acrylic acid. The tannic acid-coated cellulose nanocrystals reacted with ammonium persulfate to initiate monomer polymerization, and $ZnCl_2$ was added to form a hydrogel. The resultant capacitor

achieved an energy density of 80.5 Wh kg^{-1} and its capacity remained at 84.6% at low temperatures (Figure 15b). Additionally, the capacitor outperformed state-of-the-art flexible zinc-ion hybrid capacitors at room temperature.

Compared with traditional capacitors, supercapacitors have higher capacitance, and the storage capacity is particularly large, reaching the Farad-level capacitance. Super-capacitors store electrochemical energy primarily through surface adsorption of electrolytic ions, which are often classified as double-layer capacitors, or fast surface REDOX reactions, which can be classified as quasi capacitors.[172,176] Usually, hydrogels act as electrolytes for capacitors. Qin *et al.* designed an integrated charging energy storage system composed of super-capacitor and TENG, which was made of cellulose as raw material and based on hydrogel.[177] The hydrogel had a light transmittance of 93% and electrical conductivity of 1.92 S m^{-1}, and it was able to function normally at -54.3 ℃. Given the capability to harvest and store energy even at extremely harsh conditions, the system demonstrated potential to be exploited as a source of great power supply for applications in wearable electronic devices.

As another energy storage device, a battery typically consists of two active electrochemical electrodes separated by an ionic conductive barrier. For galvanic or rechargeable batteries, hydrogels give rigid batteries more flexibility than traditional electrode materials, which is important for flexible/stretchable batteries for wearable electronics.[145] Park *et al.* made a mixed energy storage battery (Figure 15c) using water-in-bisalt (WIBS)-soaked poly (acrylic acid) hydrogel electrolyte.[147] Due to the hierarchical porosity of nitrogen-incorporated nanoporous carbon/nanosulfur, nanoscale confinement and high ionic conductivity of WIBS hydrogels was attainable. The battery had a retention rate of 78.7% and an energy efficiency of 98% over 2000 cycles, as well as high power density and energy density. Ye *et al.* prepared the first all-hydrogel battery which was made of polyacrylamide/glycerol/carbon nanotubes (Figure 15d).[178] The dehydrated hydrogel electrode could be rehydrated by placing it in

839 contact with the hydrogel electrolyte. When the hydrogel electrolyte and the hydrogel electrode
840 reached water equilibrium, a fusion interface was formed establishing a stable all-hydrogel
841 battery under the condition of encapsulation into isolation. Since the battery was completely
842 based on hydrogel, the Young's modulus (80 kPa) of the soft battery perfectly matched with
843 human tissue. In addition, the all-hydrogel battery had a specific capacity similar to a lithium-
844 ion battery of 83 mAh g^{-1} and a specific capacity of a psychological consultation battery of 370
845 mAh g^{-1} at a current density of 0.5 A g^{-1}. Mayer *et al.* took inspiration from electric eels and
846 developed a hydrogel-based tubular system that perfectly mimics the characteristics of
847 electricity-generating cells (Figure 15e).[179] The hydrogel used in this system was synthesized
848 from acrylamide and sodium chloride. This point generation system can generate a voltage of
849 110 V with a power density of 27 mW m^{-2} per gel cell. They also carefully designed an origami-
850 like folding structure to help control the discharge, resulting in a power source that produced a
851 voltage similar to that of the eel. Rapid charge/discharge of the battery can cause a rapid rise
852 in local temperature. High operating temperatures can lead to permanent degradation of battery
853 performance and even explosion and fire risk.[180] Hence, the efficient thermal protection of
854 batteries is very critical. Yang *et al.* demonstrated an adaptive strategy to avoid thermal
855 runaway in water-based zinc-ion batteries by using a hygroscopic hydrogel electrolyte rich in
856 zinc chloride (Figure 15f).[181] The hydrogel electrolyte was formed from PAAm and zinc
857 chloride solution. When the temperature is high, the water in the electrolyte will evaporate, and
858 then the ion transport between the two electrodes will gradually slow down and eventually stop.

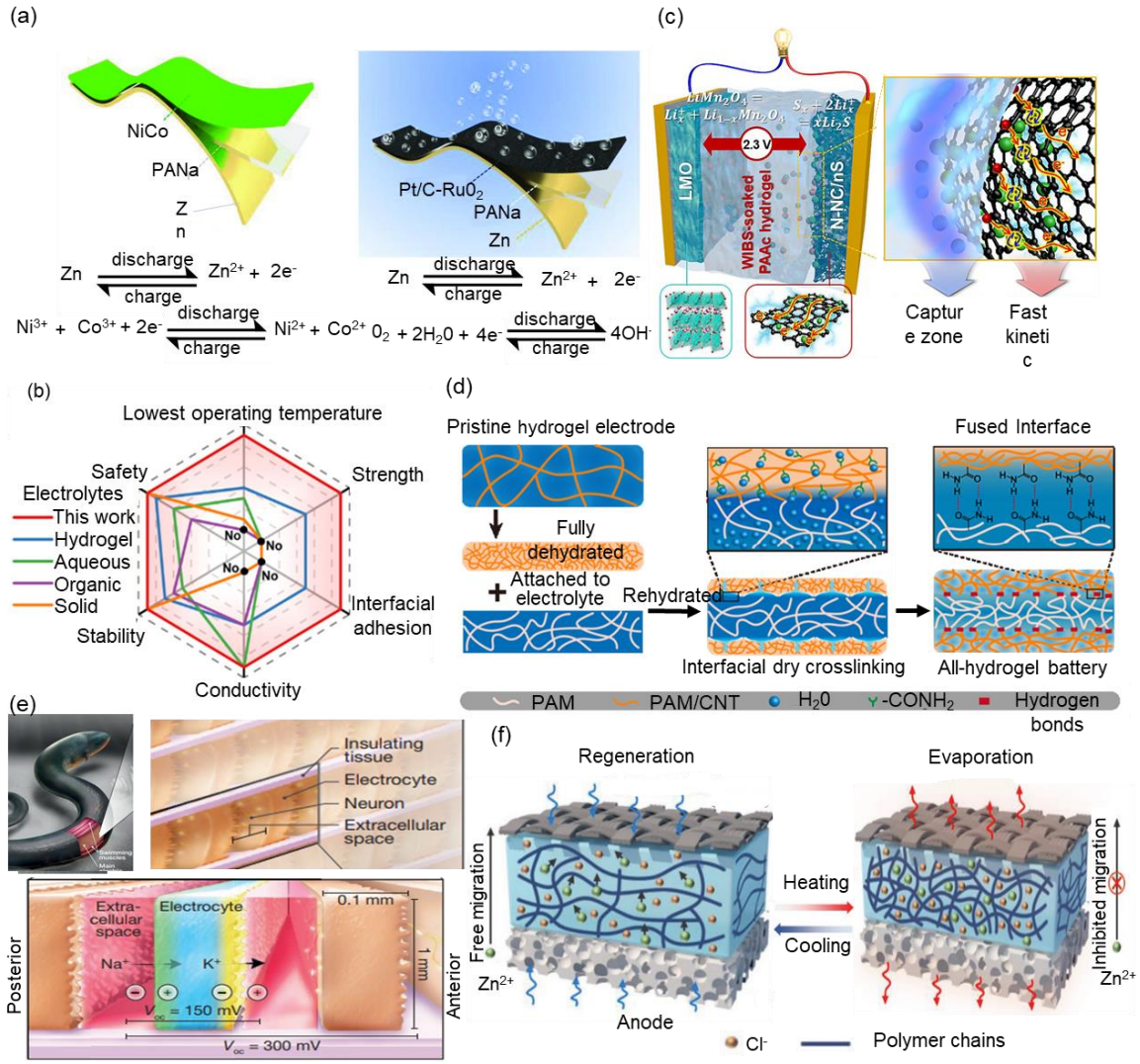

Figure 15. (a) The Zn//NiCo battery comprising the PANa polyelectrolyte, the Zn anode and the NiCoOH cathode. Electrochemical mechanism is shown underneath. The Zn-air battery comprising the sodium polyacrylate hydrogel polyelectrolyte, the Zn anode and the Pt/C-RuO_2 air cathode. Electrochemical mechanism is shown underneath. Reproduced with permission from Wiley Publications.[148] Copyright 2018. (b) Radar plots of the comprehensive performances of different electrolytes. Reproduced with permission from ACS Publications.[175] Copyright 2021. (c) Schematic of facile multivalent redox chemistries in water-in-bisalt hydrogel electrolytes for hybrid energy storage full cells. Reproduced with permission from ACS Publications.[147] Copyright 2020. (d) Preparation of interfacial dry cross-linked all-hydrogel batteries. Reproduced with permission from Wiley Publications.[178] Copyright 2021. (e) The left inset shows electrophorus electricus. The top inset shows the arrangement of electrocytes within the electric organs of electrophorus electricus. The bottom inset shows ion fluxes in the firing state. VOC, open-circuit voltage. Reproduced with permission from Nature

Publications.[179] Copyright 2017. (f) Working principle of the thermal self-protective zinc-ion batteries based on hygroscopic hydrogel electrolyte. Reproduced with permission from Wiley Publications.[181] Copyright 2020.

4.4. Actuators

An actuator is a machine or machine part that converts other forms of energy into mechanical energy to produce force and motion.[24] Actuators realize flexible motion by using the deformation of the material itself.[154] As mentioned above in this paper, the stimuli-responsive properties of hydrogels have attracted many attentions.[153] Compared with traditional materials with better mechanical properties,[150] hydrogels are flexible and more suitable for the fabrication of actuators in terms of achieving reversible motions and volume/ shape changes that are necessary for the functioning of the actuators. Hydrogels can be regulated by various stimuli such as pH,[13,182,183] light,[150,183] temperature,[105,106,152,184-188] electricity,[125,154,189-192] humidity,[193] certain chemicals,[194] magnetic field,[155,195] etc. (Figure 16). For example, Zhang *et al.* proposed a double-layer colored hydrogel actuator.[152] This type of hydrogels can expand and contract under external stimuli, enabling reversible twisting and bending. Coupling this unique property and the inherent flexibility, hydrogels can be used for grasping fragile objects,[196] engineering design in special environments,[149] etc. The hydrogel used a hybrid inverse opal scaffold to connect the polyacrylic acid-co-acrylamide layer and the poly-N-isopropylacrylamide layer together. Due to the opposite thermal response of the two hydrogels, the internal water distribution in the composite double-layer hydrogels varied during heating or cooling, which enabled the material to bend/stretch and thus achieved a series of complex motions, such as tightening, gripping, and releasing.

4.5. Transistors

Similar to the use of hydrogels for capacitor electrolytes, polyelectrolyte hydrogels can be used

to regulate ion signals.[197] When a positively charged counterions and a negatively-charged counterions gel are positioned opposite each other on the wall of an ion channel, they act as field-effect transistors. Field-effect transistors (FET) are platforms for real-time monitoring as well as achieving unlabeled transduction of biochemical signals with unprecedented sensitivity and temporal and spatial resolution. The hydrogel FET adjusts the ion signal through the gate voltage. The ionic hydrogel can be used as a dielectric material for transistors with large capacitance and high induced carrier concentration. Since hydrogels have biosimilar electrical properties, shape, and biocompatibility, ionic-gated transistors have the potential advantage of being compatible with biological signals.

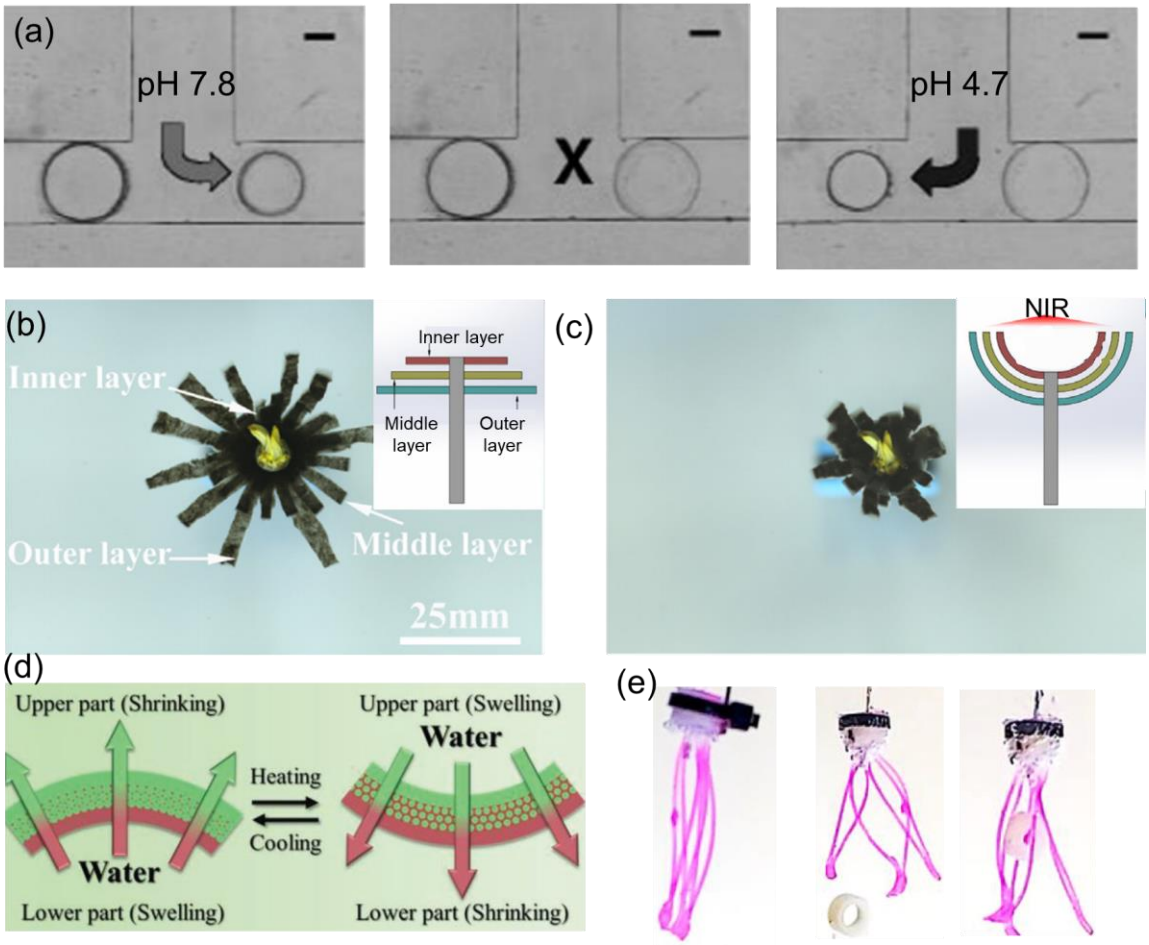

Figure 16. (a) Influence of pH on the shape of flexible hydrogels. Reproduced with permission from Nature Publications.[182] Copyright 2000. (b, c) Initial state of the bionic chrysanthemum;

closing state of the bionic chrysanthemum under NIR. Reproduced with permission from Elsevier B.V..[150] Copyright 2018. (d) Effect of temperature on the shape of irritating hydrogels. Reproduced with permission from Wiley Publications.[152] Copyright 2019. (e) Schematic of jellyfish-mimicking gripper in opening and closing states, respectively. Reproduced with permission from ACS Publications.[153] Copyright 2020.

Bay *et al.* fabricated nano-FETs using bioactive hydrogels as the gate material and selectively patterned the hydrogels on the top of a single graphene FET device using spatially limited photo-polymerization, with diffractive limited spatial resolution (Figure 17a-i).[156] Combined with microfluidic control on the chip, bio-specific detection can be achieved. Hydrogel-mediated penicillinase integration was shown to efficiently catalyze enzymatic reactions in a confined microenvironment, enabling monitoring of penicillin as low as 0.2 mM. And the multiple functionalization of acetylcholinesterase and penicillinase was shown to enable highly specific sensing (Figure 17a-ii) . Cunha *et al.* developed the cellulose based composite hydrogel electrolytes by dissolving microcrystalline cellulose in lithium hydroxide/urea aqueous solution and doping with different carboxymethyl cellulose mixing levels, and designed transistors with layered cellulose based hydrogel electrolytes as gate dielectric.[198] Using laminated cellulose-based hydrogel electrolyte as gate dielectric, the indium-gallium-zinc oxide electrolyte-gated transistors on glass had a low operating voltage (<2 V), an on-off current ratio of 106, a subthreshold swing of less than 0.2 V dec^{-1}, and a saturation mobility of 26 cm^2 V^{-1} s^{-1}. The technology showcases flexible cellulose-based hydrogel electrolyte-gated transistors with a switching frequency of up to 100 Hz. Li *et al.* developed a novel gate-free hydrogel-graphene transistor for use as an underwater microphone. [199] The hydrogel was formed by using PAAm as the main network and sodium hydroxide or sodium chloride as the ionic conductor. Due to the interaction between graphene and ions in the hydrogel, no bias was required for the formation of electric double layers, and the device worked even without a gate

electrode.

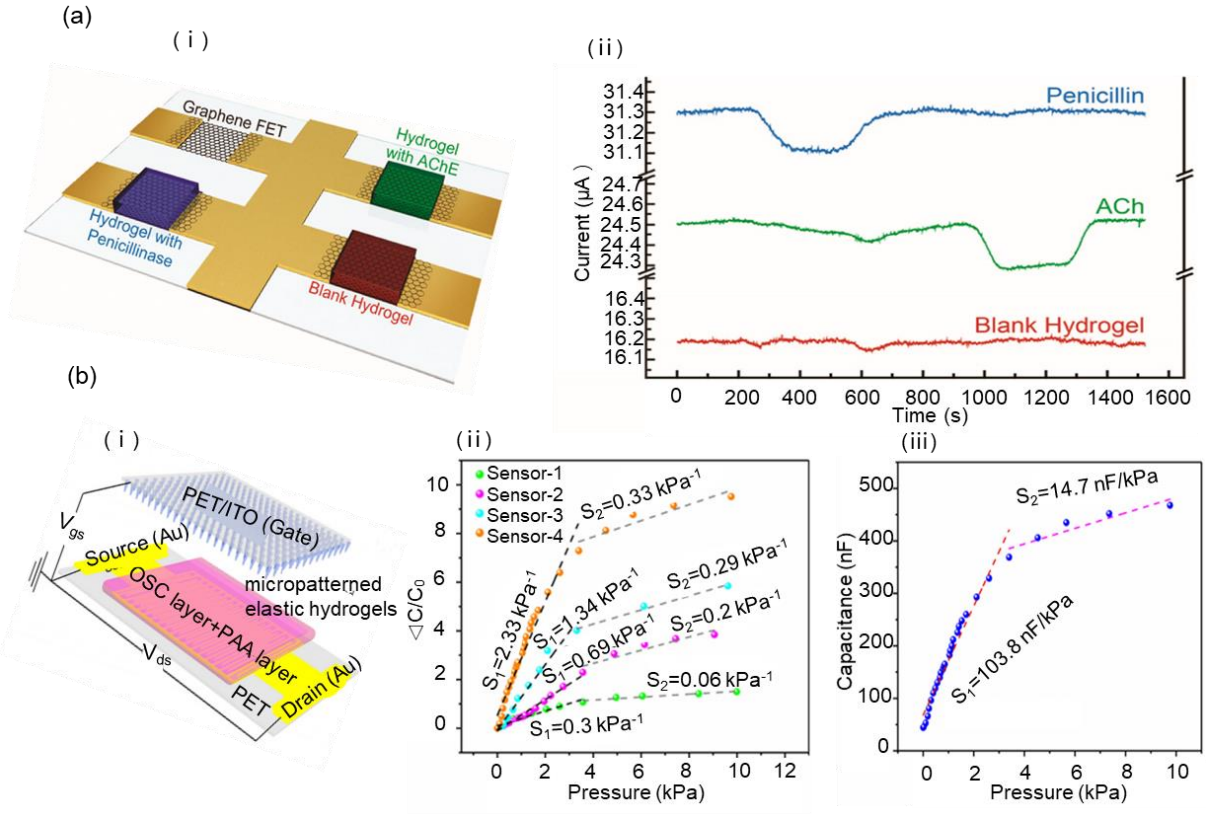

Figure 17. Schematic representation of (a) (i) graphene Nanoscale field-effect transistors device arrays with individually patterned biologically encoded hydrogel gates. Gold, electrode interconnects for the graphene field effect transistor devices. Black, graphene channels. Red, green, and blue, specifically encoded hydrogel gates. (ii) Real time multiplexed sensing of penicillin and acetylcholine chloride. Reproduced with permission from ACS Publications.[156] Copyright 2019. (b) (i) Schematic of a transistor applied to a sensor. (ii) Pressure response curves of different EIPH microstructure pressure sensors. (iii) Capacitance change in the micro-pillar structures sensor with respect to the applied pressure. Reproduced with permission from Elsevier B.V..[137] Copyright 2019.

Organic thin film transistor (OTFT) is a FET generally in the form of a thin film. Yin *et al.* developed a novel high capacitance elastic ion polyacrylamide hydrogel (EIPH).[137] Micro-patterned EIPH can be used as the dielectric layer in organic thin film transistor to manufacture low voltage OTFT pressure sensors for signal amplification and sensing mechanism

diversification (Figure 17b-i).[137,200-202] Due to the introduction of the transistor and micropillar structures, the sensitivity of the pressure sensor was greatly increased. The capacitive sensor had a 10-meter-wide EIPH micro-column structure and is more than 100 times more sensitive than the traditional capacitive pressure sensor yet operating at a low voltage (Figure 17b-ii, iii).

4.6. Electromagnetic Shielding

Electromagnetic waves are everywhere around us and affect our lives all the time. The electromagnetic interference can have negative effects on military missions or scientific experiments.[203] Electromagnetic shielding reduces electromagnetic interference by blocking electromagnetic fields with a barrier made of conductive or magnetic material that isolates electronic devices from the surrounding environment.[145] The main methods of designing high performance electromagnetic interference shielding materials focus on improving the electrical conductivity of the materials.[157] The porous network of hydrogel infilled with liquid aids with the repeated absorption and reflection of the microwave, giving hydrogels electromagnetic shielding capability.[158] Water has been widely shown to generate polarization losses and attenuate electromagnetic waves in the gigahertz and terahertz bands.[204-207] If sufficient water molecules can be immobilized in a material with moderate electrical conductivity, enhanced attenuation of the penetrating wave can be achieved without causing unnecessary reflection.[157] Conductive hydrogels with more than 90% water content have strong potential to absorb electromagnetic waves.[157,208] By adding fillers with electromagnetic shielding properties to hydrogels with ultra-high water content, the hydrogels have stronger electromagnetic shielding properties. 3D porous MXene hydrogels stand out as ideal electromagnetic interference shielding materials because they can generate more scattering centers for the electromagnetic waves reflected internally than spacer nanosheets (Figure 18a-i).[171] Most incoming microwaves are absorbed and reflected repeatedly due to the presence of porous network and water in the pores (Figure 18b). [157,158] Zhu *et al.* developed MXene and poly (acrylic acid)

hydrogel-type shielding materials.[157] Due to the combination of medium conductivity generated by porous structure, MXene network, and the internal water-rich environment, the hydrogel showed absorption-dominated electromagnetic interference shielding behavior. The hydrogel could achieve a high electromagnetic interference intensity of 45.3 dB at 0.13 mm (Figure 18a-ii). Using cellulose nanofibers as dispersant, Yang *et al.* introduced multi-walled carbon nanotubes into hydrophobic associated polyacrylamide hydrogels to prepare mechanical and electrical self-healing hydrogels with high electromagnetic interference shielding performance.[158] The hydrogel can achieve an EMI shielding effectiveness of 28.5 dB and a tensile strength of 0.24 MPa. Guand *et al.* obtained cellulose nanofiber/carbon nanotubes (CNF/CNTs) hydrogels with robust three-dimensional dual network structure by using a fast, large-scale, environmentally friendly, and low energy consumption strategy.[203] This cellulose nanofiber/carbon nanotubes material displayed the best electromagnetic interference shielding of any structural material ever reported and could potentially be exploited as a means to design electromagnetic shielding building, cars, etc. In particular, vehicles with sophisticated electrical equipment can be shielded from various electromagnetic interference up to 100 dB whereas security of electronic equipment and data inside the electromagnetic shielding buildings can be protected.[203] Liu *et al.* developed a PEDOT:PSS hydrogel by 3D printing. The hydrogel was functionalized with Ti_3C_2 MXene.[209] Despite a small thickness, the hydrogel exhibited excellent electromagnetic interference shielding performance. The hydrogel possessed a conductivity of 1525.8 S m^{-1} when the water content is above 95% (Figure 18c).

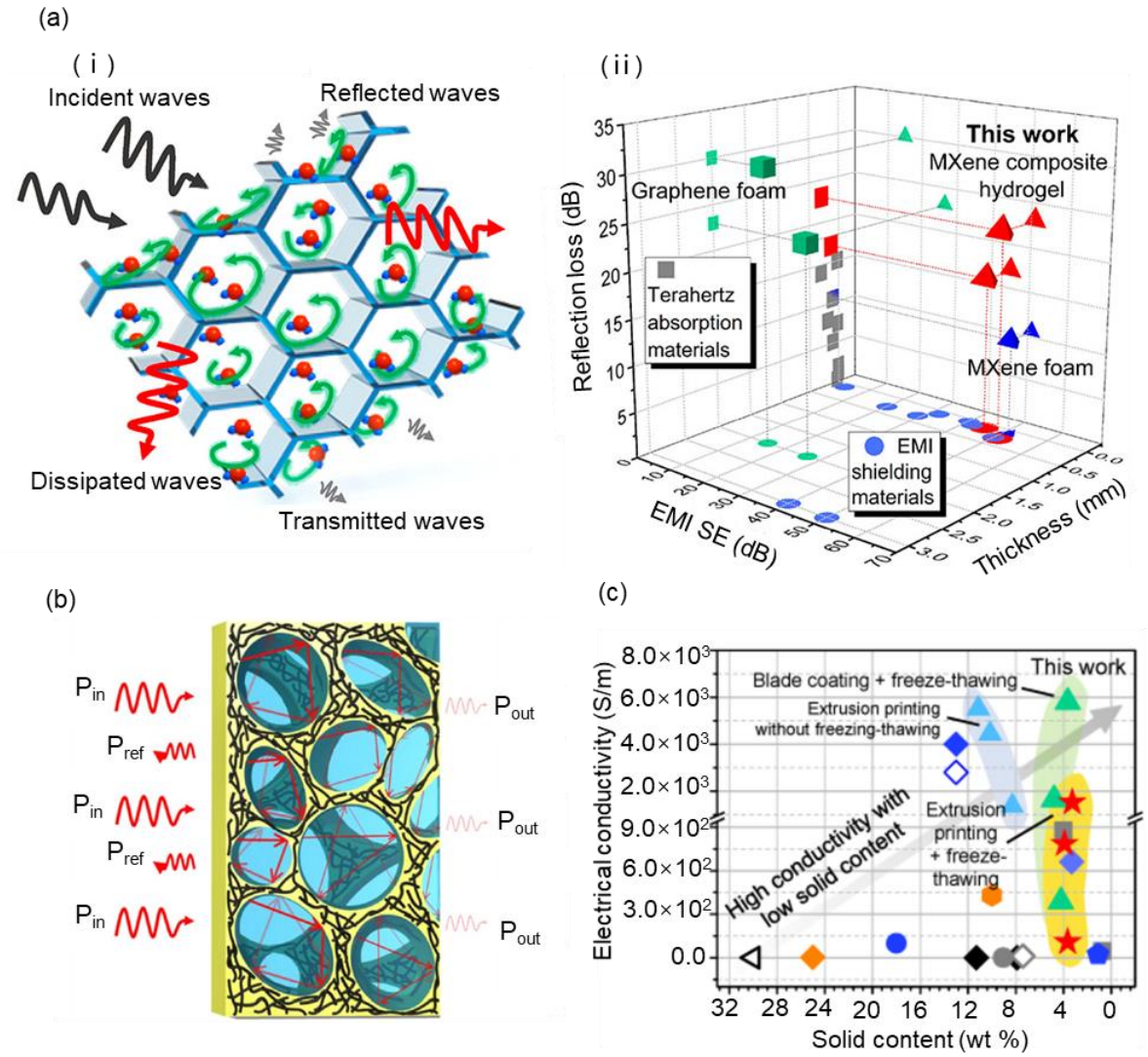

Figure 18. (a) (i) Schematic diagram of electromagnetic shielding. (a) (ii) Comparison of the terahertz shielding and absorption performances. Reproduced with permission from ACS Publications.[157] Copyright 2021. (b) Schematic of the microwaves shielding process for the composite hydrogel with various multi-walled carbon nanotubes contents. Reproduced with permission from ACS Publications.[158] Copyright 2018. (c) Comparison of the electrical conductivity as a function of solid content. Reproduced with permission from Wiley Publications.[209] Copyright 2021.

4.7. Touch Screen

Human-computer interaction has become increasingly important, and touch screen is a very popular human-computer interaction medium. Hydrogels are well equipped to function as the

interaction medium given their biocompatibility to interface with human body. In addition, the flexibility of hydrogels enables them to better attached to curved surfaces to provide high resolution. With excellent transparency (>90%), hydrogels can also transmit light information. The traditional touch screen was based on the transparent conductive film of indium tin oxide (ITO), which is hard and fragile limiting its movement and conformity to surface/human body as well as lacks the ability to repair itself after broken. In contrast, the hydrogel-based touch screen is biocompatible and flexible that is capable of conforming to the surface of the skin for maximum efficiency.[159] Hydrogel touch screen mostly uses capacitive principle to sense the touch position.[159,210] Kim *et al*. demonstrated an ionic touch panel based on a lithium-containing polyacrylamide hydrogel. The panel was soft and stretchable, so it can withstand a lot of deformation.[159] The transparent panel achieved 98% transmittance of visible light, which is an indication of free transmission of optical information. They also studied the position sensing mechanism of one-dimensional ion touchpad and applied the position sensing mechanism to a two-dimensional panel for writing text on the panel (Figure 19a). The touchpad can operate at a strain up to 1000% without sacrificing its functionality. Wang *et al.* developed a soft, self-healable, and transparent polyzwitterion–clay nanocomposite hydrogel, which can be used as a self-repairing man-machine interaction touch pad with pressure-sensitive adhesion, and had high transmittance (98.8%) and fracture strain (1500%).[210] The device used a capacitive principle to sense the position of the touch and had a sensitive perception that can sense point-by-point touch and continuous movement (Figure 19b and 19c).

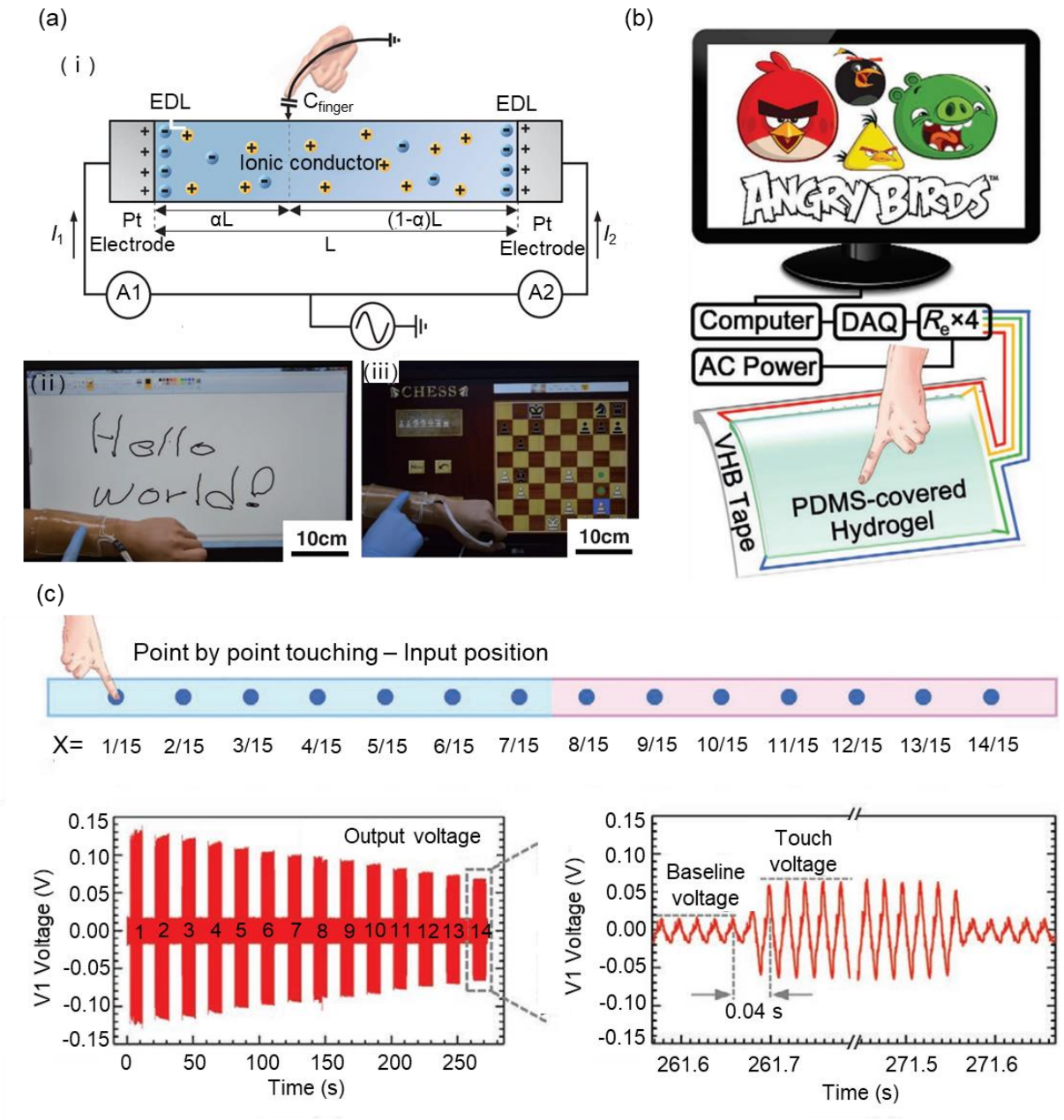

Figure 19. (a) (i) The architecture of a touch strip. The epidermal touch panel is capable of detecting motions. Demonstrations such as writing words (ii) and playing chess (iii) are shown. Reproduced with permission from Science Publications.[159] Copyright 2016. (b) A schematic diagram of a wearable touch pad integrated into a personal computer system. (c) Touch the hydrogel strip point by point with your finger and record the corresponding V_1 voltage. Reproduced with permission from Wiley Publications.[210] Copyright 2020.

4.8. Devices for Drug Controlled Release

Diabetic wound healing is a worldwide problem and a major cause of non-traumatic amputation. Despite many inspiring and interesting researches in drug controlling by detecting the change in pH,[161,211] glucose level,[211] temperature, [54] and so on, the healing of diabetic ulcers and wounds is still a challenge. The combination of wound monitoring and controlled drug release can improve the healing rate of diabetic ulcers by delivering drugs to the wound at the right time.[161]

Hydrogels used for such application has to be able to hold and release the drugs at a controlled rate, along with good biocompatibility (Table 1). The drug controlled releasing devices can transmit wound signals to electronic devices such as mobile phones through wireless transmission devices, thus realizing remote control.[54,161] By combining multiple devices, real-time monitoring, early diagnosis, and on-demand drug release can be achieved to reduce wound healing time.[54] The high water content of the hydrogels effectively alleviates the pain of the wound and provides a moist wound environment that promotes wound healing.[211] Zhu *et al.* developed an amphoteric hydrogel, which can quantitatively analyze the pH and glucose content of the wound through the color changes by reacting to the pH indicator and glucose.[211] Upon assessing the wound condition, the option of drug release will be triggered accordingly (Figure 20a). The smart hydrogel used phenol red as the pH indicator, and added two glucose-sensing enzymes, glucose oxidase and horseradish peroxidase, to polycarboxybetaine. Pang *et al.* designed an intelligent dressing that can monitor wound temperature in real time. The smart dressing had a double layer structure.[54] One layer of the structure was a polydimethylsiloxane based integrated temperature sensor and UV light-emitting diode (LED). The other layer was a hydrogel that responded to ultraviolet light. The gentamicin was covalently grafted onto polyvinyl alcohol (PVA) through a UV-cleavable linker to form a UV-responsive antibacterial hydrogel. Such work provides guidance on the treatment of wound infections through real-time temperature monitoring, thus improving wound healing efficiency and reducing antibiotic

resistance (Figure 20b). Khademhosseini *et al.* have integrated temperature and pH sensors into hydrogels to achieve an intelligent, automated, closed-loop, and on-demand drug delivery system.[161] Thermally responsive PNIPAM particles were incorporated into alginate hydrogels to form thermally responsive sheets. The PNIPAM particles were grafted or copolymerized with other substances to increase their critical temperature from 32 to 37 °C, making them suitable for topical applications such as skin where the temperature is lower than 37 °C. The system can monitor the wound state in real time and guide the release of drugs according to the healing state of the wound. Besides achieving personalized treatment, this real time monitoring of wound, and on-demand drug delivery system is very applicable for the treatment of chronic wounds that requires new dose of medication at regular intervals (Figure 20c). In this way, events of overdosage and low dosage can be avoided.

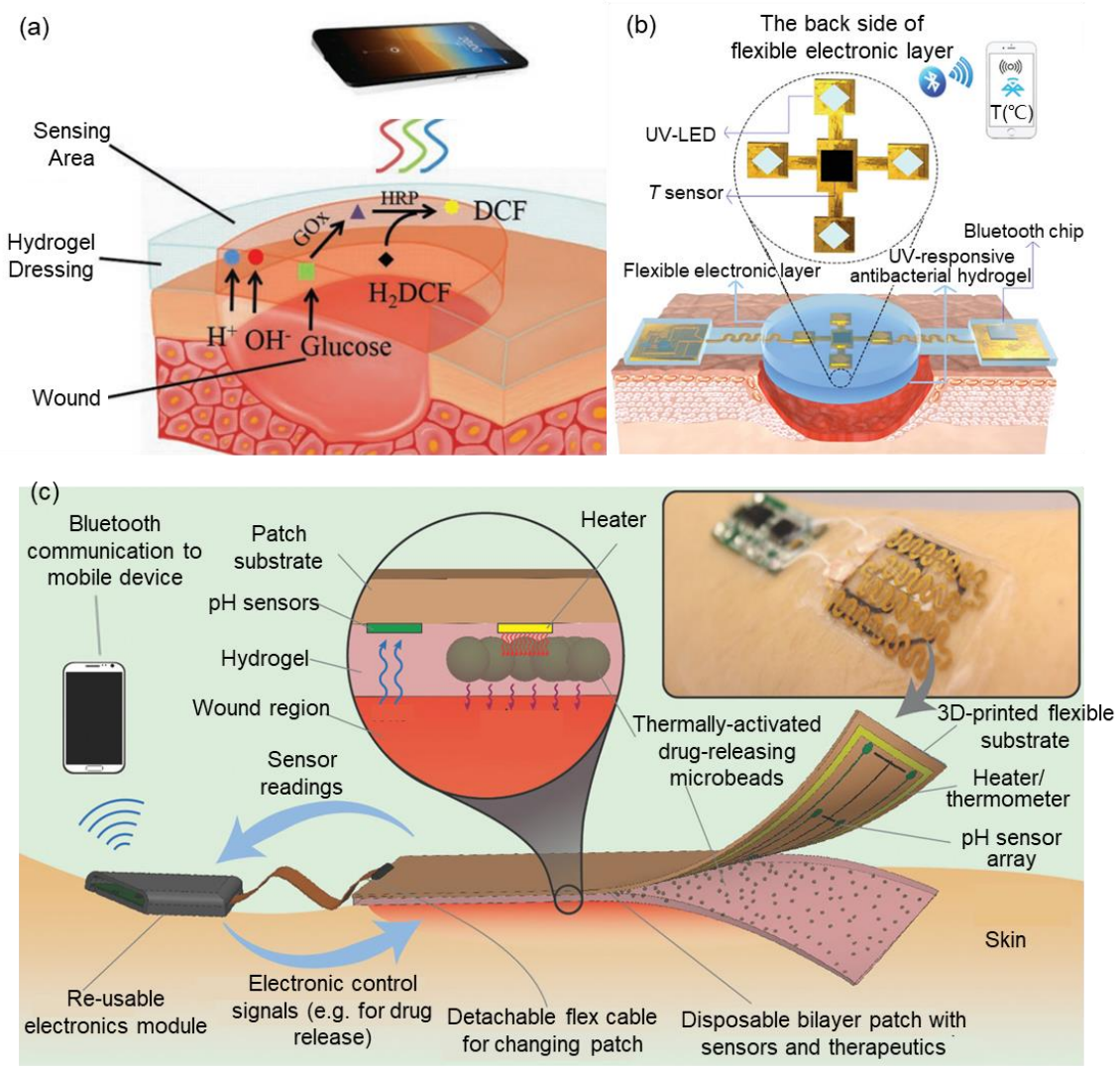

Figure 20. (a) Scheme of polycarboxybetaine hydrogel dressing for the detection of pH value and glucose concentration in wound exudate. Reproduced with permission from Wiley Publications.[211] Copyright 2019. (b) Schematics of the structures of the smart flexible electronics-integrated wound dressing. Reproduced with permission from Wiley Publications.[54] Copyright 2020. (c) Schematic and conceptual view of the automated smart bandage. Reproduced with permission from Wiley Publications.[161] Copyright 2018.

5. Conclusions and Outlook

In this review, we have summarized and highlighted recent advances in hydrogel-based flexible electronics for an array of diverse applications. As the applications of flexible electronics are

dictated by the intrinsic properties of hydrogels, the structure-based classification and stimuli-responsiveness properties of hydrogels have been first discussed. More importantly, we have elaborated on several important approaches to overcome the limitations of ordinary hydrogels as flexible electronics. Hydrogels are usually poor in conductivity, and it is impossible to directly print circuits and the like on hydrogels. To improve the conductivity of hydrogels, approaches like inclusion of conductive fillers/dopants, the selection of hydrogel made of conductive polymers, and the introduction of double-network strategy have been developed.[212] Mechanical weakness is another critical issue for the development of hydrogel-based flexible electronics. Several efforts have been made to improve the mechanical properties, e.g., the addition of fillers/dopants, the adoption of an effective energy dissipation platform, the use of anisotropic material, and the practice of hybrid system.[213] Self-healing is an important parameter for settings of electronic skins. Various methods have correspondingly been investigated for its relevance in realizing the self-healing capability and it can be categorized under two major approaches, either based on dynamic covalent bonds or noncovalent bonds. Last but not the least, there is the adhesion problem of hydrogels to other materials arising from the gradual change in hydrogel property due to evaporation of water.[214] The long-term water stability and environmental resistance of hydrogels are challenges for hydrogel-based flexible electronics. Introducing humectant and encapsulation with elastomers are some potential solutions available to address the adhesion issue.[215] There are a few methods to improve water retention, for example, using macromolecules containing more hydrophilic groups as the backbone of hydrogels, introducing some organic solvents, encapsulating hydrogels, introducing salts, etc. [212,213,215]

Despite significant progresses in developing hydrogel-based flexible electronics in the past decade, there are still several formidable challenges out there preventing hydrogel-based flexible electronics being harmonically part of our daily lives. The first challenge is the

integration of hydrogel-based flexible electronics. Currently, the functions of hydrogel-based flexible electronics remain limited and usually singular, the future model of hydrogel-based flexible electronics will be ideally multifunctional. For instance, an ideal bioelectronic device should incorporate functions of sampling, data generation and transmission, self-powered and timely interactions with humans on top of basic characteristics of flexibility, conformability, biocompatibility, and comfortability. Integration of all these functions requires creative ideas and needs to leverage on the convergence of various technology innovations. Another critical challenge is the easy tailorability and adaptability of hydrogel-based flexible electronics to meet different needs of daily life under different circumstances. More strategies should be focused on how to integrate the hydrogel devices with the biological systems, including the wearability or implantability. In term of engineering aspects, the geometry, long-term and/or temperature-related stability, and self-repairing ability of the hydrogels should be improved, apart from other functional requirements of data collection and communications. That being said, the acceleration in technology innovations and synergies, including the discoveries of new materials, explorations of new properties and functions of conventional materials,[216] revolutions in materials processing (e.g., additive manufacturing),[217] and advances in wireless communications (e.g., advanced Bluetooth or NFC communications), have brought powerful flexible electronics once only imagined in science fictions closer and closer to our daily lives.

Conflicts of interest

The authors declare no competing financial interest.

Acknowledgements

This work was financially supported by the National Key R&D Program of China

(2017YFA0204700), the Joint Research Funds of Department of Science & Technology of Shaanxi Province and Northwestern Polytechnical University (No. 2020GXLH-Z-021), and Fundamental Research Funds for the Central Universities. The authors gratefully acknowledge the financial support from CDA (Project No. CDA 202D800033) and AME Programmatic Funds (under grant A18A1b0045), Agency for Science, Technology and Research (A*STAR) and the China Scholarship Council (No. 202006290287).

References

[1] M. D. Dickey, *Adv. Mater.* **2017**, *29*, 19.

[2] R. L. Crabb, F. C. Treble, *Nature* **1967**, *213*, 1223.

[3] H. Shirakawa, E. J. Louis, A. G. Macdiarmid, C. K. Chiang, A. J. Heeger, *J. Chem. Soc. Chem. Commun.* **1977**, 578.

[4] S. H. Glarum, *J. Phys. Chem. Solids* **1963**, *24*, 1577.

[5] P. L. Kronick, M. M. Labes, *J. Chem. Phys.* **1961**, *35*, 2016.

[6] R. C. Chittick, Alexande.Jh, H. F. Sterling, *J. Electrochem. Soc.* **1969**, *116*, 77.

[7] M. Xie, Y. Zhang, M. J. Krasny, C. Bowen, H. Khanbareh, N. Gathercole, *Energy Environ. Sci.* **2018**, *11*, 2919.

[8] Y. H. Jung, S. K. Hong, H. S. Wang, J. H. Han, T. X. Pham, H. Park, J. Kim, S. Kang, C. D. Yoo, K. J. Lee, *Adv. Mater.* **2020**, *32*, 1904020.

[9] T. Q. Trung, N. E. Lee, *Adv. Mater.* **2016**, *28*, 4338.

[10] F. R. Fan, Z. Q. Tian, Z. L. Wang, *Nano Energy* **2012**, *1*, 328.

[11] F. R. Fan, W. Tang, Z. L. Wang, *Adv. Mater.* **2016**, *28*, 4283.

[12] B. Jiang, Y. Long, X. Pu, W. G. Hu, Z. L. Wang, *Nano Energy* **2021**, *86*, 8.

[13] Z. Han, P. Wang, G. Mao, T. Yin, D. Zhong, B. Yiming, X. Hu, Z. Jia, G. Nian, S. Qu, W. Yang, *ACS Appl. Mater. Interfaces* **2020**, *12*, 12010.

[14] M. Yao, R. Wang, Z. Zhao, Y. Liu, Z. Niu, J. Chen, *ACS Nano* **2018**, *12*, 12503.

[15] N. Li, Q. Wang, C. Shen, Z. Wei, H. Yu, J. Zhao, X. Lu, G. Wang, C. He, L. Xie, J. Zhu, L. Du, R. Yang, D. Shi, G. Zhang, *Nat. Electron.* **2020**, *3*, 711.

[16] T. Sekitani, T. Yokota, U. Zschieschang, H. Klauk, S. Bauer, K. Takeuchi, M. Takamiya, T. Sakurai, T. Someya, *Science* **2009**, *326*, 1516.

[17] A. Liu, H. H. Zhu, W. T. Park, S. J. Kang, Y. Xu, M. G. Kim, Y. Y. Noh, *Adv. Mater.* **2018**, *30*, 7.

[18] K. Y. Lee, D. J. Mooney, *Chem. Rev.* **2001**, *101*, 1869.

[19] H. Fukagawa, T. Sasaki, T. Tsuzuki, Y. Nakajima, T. Takei, G. Motomura, M. Hasegawa, K. Morii, T. Shimizu, *Adv. Mater.* **2018**, *30*, 7.

[20] J. Guo, Y. Yu, L. Cai, Y. Wang, K. Shi, L. Shang, J. Pan, Y. Zhao, *Mater. Today* **2021**, *44*, 105.

[21] J. Heikenfeld, A. Jajack, J. Rogers, P. Gutruf, L. Tian, T. Pan, R. Li, M. Khine, J. Kim, J. Wang, J. Kim, *Lab on a Chip* **2018**, *18*, 217.

[22] T. R. Ray, J. Choi, A. J. Bandodkar, S. Krishnan, P. Gutruf, L. M. Tian, R. Ghaffari, J.

A. Rogers, *Chem. Rev.* **2019**, *119*, 5461.
[23] Y. R. Yang, W. Gao, *Chem. Soc. Rev.* **2019**, *48*, 1465.
[24] X. Liu, J. Liu, S. Lin, X. Zhao, *Mater. Today* **2020**, *36*, 102.
[25] X. Zhao, *Soft Matter* **2014**, *10*, 672.
[26] O. Wichterle, D. Lim, *Nature* **1960**, *185*, 117.
[27] B. Xue, H. Sheng, Y. Li, L. Li, W. Di, Z. Xu, L. Ma, X. Wang, H. Jiang, M. Qin, *Natl. Sci. Rev.* **2021**, nwab147. https://doi.org/10.1093/nsr/nwab147.
[28] S. Lin, H. Yuk, T. Zhang, G. A. Parada, H. Koo, C. Yu, X. Zhao, *Adv. Mater.* **2016**, *28*, 4497.
[29] T. Someya, Z. Bao, G. G. Malliaras, *Nature* **2016**, *540*, 379.
[30] X. Han, G. Xiao, Y. Wang, X. Chen, G. Duan, Y. Wu, X. Gong, H. Wang, *J. Mater. Chem. A* **2020**, *8*, 23059.
[31] Z. Deng, R. Yu, B. Guo, *Mater. Chem. Front.* **2021**, *5*, 2092.
[32] D. A. Gyles, L. D. Castro, J. O. C. Silva, R. M. R. Costa, *Eur. Polym. J.* **2017**, *88*, 373.
[33] Y. Tang, L. Zhen, J. Liu, J. Wu, *Anal Chem* **2013**, *85*, 2787.
[34] C. Vasile, D. Pamfil, E. Stoleru, M. Baican, *Molecules* **2020**, *25*, 1539.
[35] Z. Ren, T. Ke, Q. Ling, L. Zhao, H. Gu, *Carbohydr. Polym.* **2021**, *273*, 118533.
[36] Y. L. Jiang, Y. T. Yang, X. Y. Zheng, Y. Yi, X. C. Chen, Y. B. Li, D. Sun, L. Zhang, *NPG Asia Mater.* **2020**, *12*, 11.
[37] L. Voorhaar, R. Hoogenboom, *Chem. Soc. Rev.* **2016**, *45*, 4013.
[38] S. S. Li, Y. Z. Xia, Y. Qiu, X. N. Chen, S. X. Shi, *J. Appl. Polym. Sci.* **2018**, *135*, 13.
[39] D. Ye, C. Chang, L. Zhang, *Biomacromolecules* **2019**, *20*, 1989.
[40] T. Trimaille, V. Pertici, D. Gigmes, *C. R. Chim.* **2016**, *19*, 157.
[41] R. A. I. Azzam, *Commun. Soil Sci. Plant Anal.* **1980**, *11*, 767.
[42] Zorrato, N.; Matricardi, P. Semi-IPN- and IPN-based hydrogels. *Adv. Exp. Med. Biol.* **2018**, 1059, 155.
[43] M. Bahram, N. Mohseni, M. Moghtader, In *Emerging Concepts in Analysis and Applications of Hydrogels* **2016***,* 266.
[44] S. Ishikawa, K. Iijima, D. Matsukuma, Y. Asawa, K. Hoshi, S. Osawa, H. Otsuka, *Chem. Mater.* **2020**, *32*, 2353.
[45] T. Ren, J. Gan, L. P. Zhou, H. Chen, *Polymers* **2020**, *12*, 13.
[46] R. Censi, C. Casadidio, S. Y. Deng, M. R. Gigliobianco, M. G. Sabbieti, D. Agas, F. Laus, P. Di Martino, *Int. J. Mol. Sci.* **2020**, *21*, 16.
[47] F. Ye, M. Li, D. Ke, L. Wang, Y. Lu, *Adv. Mater. Technol.* **2019**, *4*, 1900346.

[48] M. T. Cook, P. Haddow, S. B. Kirton, W. J. McAuley, *Adv. Funct. Mater.* **2021**, *31*, 25.
[49] C. H. Zheng, H. Z. Gao, D. P. Yang, M. H. Liu, H. W. Cheng, Y. L. Wu, X. J. Loh, *Mater. Sci. Eng. C-Mater. Biol. Appl.* **2017**, *74*, 110.
[50] K. Matsumoto, N. Sakikawa, T. Miyata, *Nat. Commun.* **2018**, *9*, 7.
[51] Y. Luo, W. Li, Q. Lin, F. Zhang, K. He, D. Yang, X. J. Loh, X. Chen, *Adv. Mater.* **2021**, *33*, 2007848.
[52] L. Li, J. M. Scheiger, P. A. Levkin, *Adv. Mater.* **2019**, *31*, 17.
[53] B. J. Jiang, X. T. Liu, C. Yang, Z. G. Yang, J. R. Luo, S. Z. Kou, K. Liu, F. Sun, *Sci. Adv.* **2020**, *6*, 9.
[54] Q. Pang, D. Lou, S. Li, G. Wang, B. Qiao, S. Dong, L. Ma, C. Gao, Z. Wu, *Adv. Sci.* **2020**, *7*, 1902673.
[55] Q. Liu, L. Liu, *Langmuir* **2019**, *35*, 1450.
[56] A. Onaciu, R. A. Munteanu, A. I. Moldovan, C. S. Moldovan, I. B. Neagoe, *Pharmaceutics* **2019**, *11*, 432.
[57] H. Guo, Y. Uehara, T. Matsuda, R. Kiyama, L. Li, J. Ahmed, Y. Katsuyama, T. Nonoyama, T. Kurokawa, *Soft Matter* **2020**, *16*, 1897.
[58] J. Tang, T. Katashima, X. Li, Y. Mitsukami, Y. Yokoyama, N. Sakumichi, U.-i. Chung, M. Shibayama, T. Sakai, *Macromolecules* **2020**, *53*, 8244.
[59] I. Ali, L. Xudong, C. Xiaoqing, J. Zhiwei, M. Pervaiz, Y. Weimin, L. Haoyi, M. Sain, *Mater. Sci. Eng. C* **2019**, *103*, 109852.
[60] H. Jiang, L. Fan, S. Yan, F. Li, H. Li, J. Tang, *Nanoscale* **2019**, *11*, 2231.
[61] S. Bashir, M. Hina, J. Iqbal, A. H. Rajpar, M. A. Mujtaba, N. A. Alghamdi, S. Wageh, K. Ramesh, S. Ramesh, *Polymers* **2020**, *12*, 2702.
[62] Z. Han, P. Wang, G. Mao, T. Yin, D. Zhong, B. Yiming, X. Hu, Z. Jia, G. Nian, S. Qu, W. Yang, *ACS Appl. Mater. Interfaces* **2020**, *12*, 12010.
[63] T. Wang, X. Zhang, Z. Wang, X. Zhu, J. Liu, X. Min, T. Cao, X. Fan, *Polymers* **2019**, *11*, 1564.
[64] H. Xu, Y. Xie, E. Zhu, Y. Liu, Z. Shi, C. Xiong, Q. Yang, *J. Mater. Chem. A* **2020**, *8*, 6311.
[65] C. Arndt, M. Hauck, I. Wacker, B. Z. Plumhoff, F. Rasch, M. Taale, A. S. Nia, X. Feng, R. Adelung, R. R. Schröder, F. Schütt, C. S. Unkel, *Nano Letters* **2021**, *21*, 3690.
[66] J. Chatterjee, T. Liu, B. Wang, J. P. Zheng, *Solid State Ionics* **2010**, *181*, 531.
[67] C. Yang, P. Zhang, A. Nautiyal, S. Li, N. Liu, J. Yin, K. Deng, X. Zhang, *ACS Appl. Mater. Interfaces* **2019**, *11*, 4258.

[68] M. Moussa, M. F. E. Kady, D. Dubal, T. T. Tung, M. J. Nine, N. Mohamed, R. B. Kaner, D. Losic, *ACS Appl. Energy Mater.* **2020**, *3*, 923.
[69] H. Guo, W. He, Y. Lu, X. Zhang, *Carbon* **2015**, *92*, 133.
[70] Z. Wu, L. Rong, J. Yang, Y. Wei, K. Tao, Y. Zhou, B. R. Yang, X. Xie, J. Wu, *Small* **2021**, *17*, 2104997.
[71] Z. Wu, W. Shi, H. Ding, B. Zhong, W. Huang, Y. Zhou, X. Gui, X. Xie, J. Wu, *J. Mater. Chem. C* **2021**, *9*, 13668.
[72] S. Zhang, Y. Zhang, B. Li, P. Zhang, L. Kan, G. Wang, H. Wei, X. Zhang, N. Ma, *ACS Appl. Mater. Interfaces* **2019**, *11*, 32441.
[73] N. Sun, F. Lu, Y. Yu, L. Su, X. Gao, L. Zheng, *ACS Appl. Mater. Interfaces* **2020**, *12*, 11778.
[74] X. Yin, Y. Zhang, Q. Guo, X. Cai, J. Xiao, Z. Ding, J. Yang, *ACS Appl. Mater. Interfaces* **2018**, *10*, 10998.
[75] L. Han, L. Yan, M. Wang, K. Wang, L. Fang, J. Zhou, J. Fang, F. Ren, X. Lu, *Chem. Mater.* **2018**, *30*, 5561.
[76] C. Tondera, T. F. Akbar, A. K. Thomas, W. Lin, C. Werner, V. Busskamp, Y. Zhang, I. R. Minev, *Small* **2019**, *15*, 1901406.
[77] Z. Wang, H. Zhou, J. Lai, B. Yan, H. Liu, X. Jin, A. Ma, G. Zhang, W. Zhao, W. Chen, *J. Mater. Chem. C* **2018**, *6*, 9200.
[78] Y. Zhou, H. Li, J. Liu, Y. Xu, Y. Wang, H. Ren, X. Li, *Polym. Adv. Technol.* **2019**, *30*, 143.
[79] Y. Wang, J. Zhang, C. Qiu, J. Li, Z. Cao, C. Ma, J. Zheng, G. Huang, *Carbohydr. Polym.* **2018**, *196*, 82.
[80] M. M. Song, Y. M. Wang, B. Wang, X. Y. Liang, Z. Y. Chang, B. J. Li, S. Zhang, *ACS Appl. Mater. Interfaces* **2018**, *10*, 15021.
[81] A. Nakayama, A. Kakugo, J. P. Gong, Y. Osada, M. Takai, T. Erata, S. Kawano, *Adv. Funct. Mater.* **2004**, *14*, 1124.
[82] J.-Y. Sun, X. Zhao, W. R. Illeperuma, O. Chaudhuri, K. H. Oh, D. J. Mooney, J. J. Vlassak, Z. Suo, *Nature* **2012**, *489*, 133.
[83] Z. W. Low, P. L. Chee, D. Kai, X. J. Loh, *Rsc Advances* **2015**, *5*, 57678.
[84] Z. Ding, G. Lu, W. Cheng, G. Xu, B. Zuo, Q. Lu, D. L. Kaplan, *ACS Biomater. Sci. Eng.* **2020**, *6*, 2357.
[85] T. Nonoyama, Y. W. Lee, K. Ota, K. Fujioka, W. Hong, J. P. Gong, *Adv. Mater.* **2020**, *32*, 1905878.

[86] Q. He, Y. Huang, S. Wang, *Adv. Funct. Mater.* **2018**, *28*, 1705069.
[87] J. Wei, Q. Wang, *Small Methods* **2019**, *3*, 1900558.
[88] A. Sugawara, T. A. Asoh, Y. Takashima, A. Harada, H. Uyama, *Polym. Degrad. Stabil.* **2020**, *177*, 109157.
[89] S. Choi, Y. Choi, J. Kim, *Adv. Funct. Mater.* **2019**, *29*, 1904342.
[90] M. Hua, S. Wu, Y. Ma, Y. Zhao, Z. Chen, I. Frenkel, J. Strzalka, H. Zhou, X. Zhu, X. He, *Nature* **2021**, *590*, 594.
[91] K. Song, W. Zhu, X. Li, Z. Yu, *Mater. Lett.* **2020**, *260*, 126884.
[92] Z. Wei, J. H. Yang, Z. Q. Liu, F. Xu, J. X. Zhou, M. Zrínyi, Y. Osada, Y. M. Chen, *Adv. Funct. Mater.* **2015**, *25*, 1352.
[93] Z. X. Zhang, S. S. Liow, K. Xue, X. Zhang, Z. Li, X. J. Loh, *ACS Appl. Polym. Mater.* **2019**, *1*, 1769.
[94] Y. Wang, Y. Yu, J. Guo, Z. Zhang, X. Zhang, Y. Zhao, *Adv. Funct. Mater.* **2020**, *30*, 2000151.
[95] J. W. Kim, S. Kim, Y. R. Jeong, J. Kim, D. S. Kim, K. Keum, H. Lee, J. S. Ha, *Chem. Eng. J.* **2022**, *430*, 132685.
[96] W. Cui, M. H. Pi, Y. S. Li, L. Y. Shi, R. Ran, *ACS Appl. Polym. Mater.* **2020**, *2*, 3378.
[97] G. Gao, F. Yang, F. Zhou, J. He, W. Lu, P. Xiao, H. Yan, C. Pan, T. Chen, Z. L. Wang, *Adv. Mater.* **2020**, *32*, 2004290.
[98] L. Fang, J. Zhang, W. Wang, Y. Zhang, F. Chen, J. Zhou, F. Chen, R. Li, X. Zhou, Z. Xie, *ACS Appl. Mater. Interfaces* **2020**, *12*, 56393.
[99] D. Buenger, F. Topuz, J. Groll, *Prog. Polym. Sci.* **2012**, *37*, 1678.
[100] L. Wang, T. Xu, X. Zhang, *Trends Anal. Chem.* **2021**, *134*, 116130.
[101] Y. Gao, S. Gu, F. Jia, G. Gao, *J. Mater. Chem. A* **2020**, *8*, 24175.
[102] M. Sepantafar, R. Maheronnaghsh, H. Mohammadi, F. Radmanesh, M. M. Hasani-Sadrabadi, M. Ebrahimi, H. Baharvand, *Trends Biotechnol.* **2017**, *35*, 1074.
[103] A. Richter, G. Paschew, S. Klatt, J. Lienig, K. F. Arndt, H. J. P. Adler, *Sensors* **2008**, *8*, 561.
[104] S. R. Perera, A. Taheri, N. H. Khan, R. P. Parti, S. Stefura, P. Skiba, J. P. Acker, I. Martin, A. Kusalik, J.-A. R. Dillon, *Antibiotics* **2018**, *7*, 70.
[105] L. Dong, A. K. Agarwal, D. J. Beebe, H. Jiang, *Nature* **2006**, *442*, 551.
[106] X. H. Li, C. Liu, S. P. Feng, N. X. Fang, *Joule* **2019**, *3*, 290.
[107] W. Yu, O. Deschaume, L. Dedroog, C. J. Garcia Abrego, P. Zhang, J. Wellens, Y. de Coene, S. Jooken, K. Clays, W. Thielemans, *Adv. Funct. Mater.* **2022**, *32*, 2108234.

[108] Z. Lei, P. Wu, *Nat. Commun.* **2019**, *10*, 3429.
[109] Y. Lee, W. J. Song, J. Y. Sun, *Mater. Today Phys.* **2020**, *15*, 100258.
[110] W. Yu, O. Deschaume, L. Dedroog, C. J. G. Abrego, P. Zhang, J. Wellens, Y. D. Coene, S. Jooken, K. Clays, W. Thielemans, C. Glorieux, C. Bartic, *Adv. Funct. Mater.* **2022**, *32*, 2108234.
[111] A. Shastri, L. M. McGregor, Y. Liu, V. Harris, H. Nan, M. Mujica, Y. Vasquez, A. Bhattacharya, Y. Ma, M. Aizenberg, O. Kuksenok, A. C. Balazs, J. Aizenberg, X. He, *Nat. Chem.* **2015**, *7*, 447.
[112] T. Miyata, N. Asami, T. Uragami, *Nature* **1999**, *399*, 766.
[113] A. Tamayol, M. Akbari, Y. Zilberman, M. Comotto, E. Lesha, L. Serex, S. Bagherifard, Y. Chen, G. Fu, S. K. Ameri, W. Ruan, E. L. Miller, M. R. Dokmeci, S. Sonkusale, A. Khademhosseini, *Adv. Healthcare Mater.* **2016**, *5*, 711.
[114] Z. Xu, J. Song, B. Liu, S. Lv, F. Gao, X. Luo, P. Wang, *Sens. Actuators B Chem.* **2021**, *348*, 130674.
[115] K. H. Lee, Y. Z. Zhang, H. Kim, Y. Lei, S. Hong, S. Wustoni, A. Hama, S. Inal, H. N. Alshareef, *Small Methods* **2021**, *5*, 2100819.
[116] J. Y. Sun, C. Keplinger, G. M. Whitesides, Z. Suo, *Adv. Mater.* **2014**, *26*, 7608.
[117] Z. Lei, Q. Wang, P. Wu, *Mater. Horiz.* **2017**, *4*, 694.
[118] S. H. Shin, W. Lee, S. M. Kim, M. Lee, J. M. Koo, S. Y. Hwang, D. X. Oh, J. Park, *Chem. Eng. J.* **2019**, *371*, 452.
[119] Z. Lei, Q. Wang, S. Sun, W. Zhu, P. Wu, *Adv. Mater.* **2017**, *29*, 1700321.
[120] F. Zhan, Z. Wang, T. Wu, Q. Dong, C. Zhao, G. Wang, J. Qiu, *J. Mater. Chem. A* **2018**, *6*, 4981.
[121] Z. Shen, X. Zhu, C. Majidi, G. Gu, *Adv. Mater.* **2021**, *33*, 2102069.
[122] Z. Deng, Y. Guo, X. Zhao, P. X. Ma, B. Guo, *Chem. Mater.* **2018**, *30*, 1729.
[123] Z. Deng, T. Hu, Q. Lei, J. He, P. X. Ma, B. Guo, *ACS Appl. Mater. Interfaces* **2019**, *11*, 6796.
[124] C. Yang, Z. Suo, *Nat. Rev. Mater.* **2018**, *3*, 125.
[125] C. Keplinger, J. Y. Sun, C. C. Foo, P. Rothemund, G. M. Whitesides, Z. Suo, *Science* **2013**, *341*, 984.
[126] S. Cai, B. Niu, X. Ma, S. Wan, X. He, *Chem. Eng. J.* **2022**, *430*, 132957.
[127] S. Y. Zheng, S. Mao, J. Yuan, S. Wang, X. He, X. Zhang, C. Du, D. Zhang, Z. L. Wu, J. Yang, *Chem. Mater.* **2021**, *33*, 8418.
[128] S. Zheng, H. Wang, P. Das, Y. Zhang, Y. Cao, J. Ma, S. Liu, Z.-S. Wu, *Adv. Mater.* **2021**,

33, 2005449.

[129] G. Lin, M. Si, L. Wang, S. Wei, W. Lu, H. Liu, Y. Zhang, D. Li, T. Chen, *Adv. Opt. Mater.* **2022**, *10*, 2102306.

[130] W. Ye, Q. Cao, X. F. Cheng, C. Yu, J. H. He, J. M. Lu, *J. Mater. Chem. A* **2020**, *8*, 17675.

[131] J. Wu, Z. Wu, H. Xu, Q. Wu, C. Liu, B. R. Yang, X. Gui, X. Xie, K. Tao, Y. Shen, J. Miao, L. K. Norford, *Mater. Horiz.* **2019**, *6*, 595.

[132] F. Garciagolding, M. Giallorenzo, N. Moreno, V. Chang, *Sens. Actuators A Phys.* **1995**, *47*, 337.

[133] Y. Gao, F. Jia, G. Gao, *Chem. Eng. J.* **2022**, *430*, 132919.

[134] J. Yu, Y. Feng, D. Sun, W. Ren, C. Shao, R. Sun, *ACS Appl. Mater. Interfaces* **2022**, *14*, 10886.

[135] H. Chen, J. Huang, J. Liu, J. Gu, J. Zhu, B. Huang, J. Bai, J. Guo, X. Yang, L. Guan, *J. Mater. Chem. A* **2021**, *9*, 23243.

[136] Q. Zhang, Y. Jiang, L. Chen, W. Chen, J. Li, Y. Cai, C. Ma, W. Xu, Y. Lu, X. Jia, Z. Bao, *Adv. Funct. Mater.* **2021**, *31*, 2100686.

[137] M. J. Yin, Z. Yin, Y. Zhang, Q. Zheng, A. P. Zhang, *Nano Energy* **2019**, *58*, 96.

[138] J. H. Kwon, Y. M. Kim, H. C. Moon, *ACS Nano* **2021**, *15*, 15132.

[139] Z. Shen, X. Zhu, C. Majidi, G. Gu, *Adv. Mater.* **2021**, *33*, 2102069.

[140] X. Pei, H. Zhang, Y. Zhou, L. Zhou, J. Fu, *Mater. Horiz.* **2020**, *7*, 1872.

[141] W. Xu, L. B. Huang, M. C. Wong, L. Chen, G. Bai, J. Hao, *Adv. Energy Mater.* **2017**, *7*, 1601529.

[142] H. Sun, Y. Zhao, S. Jiao, C. Wang, Y. Jia, K. Dai, G. Zheng, C. Liu, P. Wan, C. Shen, *Adv. Funct. Mater.* **2021**, *31*, 2101696.

[143] D. Bao, Z. Wen, J. Shi, L. Xie, H. Jiang, J. Jiang, Y. Yang, W. Liao, X. Sun, *J. Mater. Chem. A* **2020**, *8*, 13787.

[144] B. Jiang, Y. Long, X. Pu, W. Hu, Z. L. Wang, *Nano Energy* **2021**, *86*, 106086.

[145] Y. Z. Zhang, J. K. E. Demellawi, Q. Jiang, G. Ge, H. Liang, K. Lee, X. Dong, H. N. Alshareef, *Chem. Soc. Rev.* **2020**, *49*, 7229.

[146] Z. Zhang, L. He, C. Zhu, Y. Qian, L. Wen, L. Jiang, *Nat. Commun.* **2020**, *11*, 875.

[147] J. M. Park, M. Jana, P. Nakhanivej, B. K. Kim, H. S. Park, *ACS Energy Lett.* **2020**, *5*, 1054.

[148] Y. Huang, Z. Li, Z. Pei, Z. Liu, H. Li, M. Zhu, J. Fan, Q. Dai, M. Zhang, L. Dai, *Adv. Energy Mater.* **2018**, *8*, 1802288.

[149] D. J. Beebe, J. S. Moore, J. M. Bauer, Q. Yu, R. H. Liu, C. Devadoss, B.-H. Jo, *Nature*

2000, *404*, 588.
[150] Q. Zhao, Y. Liang, L. Ren, Z. Yu, Z. Zhang, L. Ren, *Nano Energy* **2018**, *51*, 621.
[151] H. Qin, T. Zhang, N. Li, H. P. Cong, S. H. Yu, *Nat. Commun.* **2019**, *10*, 2202.
[152] Z. Zhang, Z. Chen, Y. Wang, J. Chi, Y. Wang, Y. Zhao, *Small Methods* **2019**, *3*, 1900519.
[153] X. Duan, J. Yu, Y. Zhu, Z. Zheng, Q. Liao, Y. Xiao, Y. Li, Z. He, Y. Zhao, H. Wang, L. Qu, *ACS Nano* **2020**, *14*, 14929.
[154] D. Han, C. Farino, C. Yang, T. Scott, D. Browe, W. Choi, J. W. Freeman, H. Lee, *ACS Appl. Mater. Interfaces* **2018**, *10*, 17512.
[155] X. Zhao, J. Kim, C. A. Cezar, N. Huebsch, K. Lee, K. Bouhadir, D. J. Mooney, *Proc. Natl. Acad. Sci. U.S.A.* **2011**, *108*, 67.
[156] H. H. Bay, R. Vo, X. Dai, H. H. Hsu, Z. Mo, S. Cao, W. Li, F. G. Omenetto, X. Jiang, *Nano Lett.* **2019**, *19*, 2620.
[157] Y. Zhu, J. Liu, T. Guo, J. J. Wang, X. Tang, V. Nicolosi, *ACS Nano* **2021**, *15*, 1465.
[158] W. Yang, B. Shao, T. Liu, Y. Zhang, R. Huang, F. Chen, Q. Fu, *ACS Appl. Mater. Interfaces* **2018**, *10*, 8245.
[159] C. C. Kim, H. H. Lee, K. H. Oh, J. Y. Sun, *Science* **2016**, *353*, 682.
[160] Y. Zhu, J. Zhang, J. Song, J. Yang, Z. Du, W. Zhao, H. Guo, C. Wen, Q. Li, X. Sui, L. Zhang, *Adv. Funct. Mater.* **2020**, *30*, 1905493.
[161] P. Mostafalu, A. Tamayol, R. Rahimi, M. Ochoa, A. Khalilpour, G. Kiaee, I. K. Yazdi, S. Bagherifard, M. R. Dokmeci, B. Ziaie, *Small* **2018**, *14*, 1703509.
[162] T. Ma, E. Balanzat, J. M. Janot, S. Balme, *ACS Appl. Mater. Interfaces* **2019**, *11*, 12578.
[163] Y. Guo, J. Bae, Z. Fang, P. Li, F. Zhao, G. Yu, *Chem. Rev.* **2020**, *120*, 7642.
[164] Q. Hua, J. Sun, H. Liu, R. Bao, R. Yu, J. Zhai, C. Pan, Z. L. Wang, *Nat. Commun.* **2018**, *9*, 244.
[165] Z. Wu, B. Zhang, H. Zou, Z. Lin, G. Liu, Z. L. Wang, *Adv. Energy Mater.* **2019**, *9*, 1901124.
[166] Z. Xu, F. Zhou, H. Yan, G. Gao, H. Li, R. Li, T. Chen, *Nano Energy* **2021**, *90*, 106614.
[167] H. Sun, Y. Zhao, C. Wang, K. Zhou, C. Yan, G. Zheng, J. Huang, K. Dai, C. Liu, C. Shen, *Nano Energy* **2020**, *76*, 105035.
[168] L. Yang, D. K. Nandakumar, L. Miao, L. Suresh, D. Zhang, T. Xiong, J. V. Vaghasiya, K. C. Kwon, S. Ching Tan, *Joule* **2020**, *4*, 176.
[169] S. Pu, Y. Liao, K. Chen, J. Fu, S. Zhang, L. Ge, G. Conta, S. Bouzarif, T. Cheng, X. Hu, K. Liu, J. Chen, *Nano Lett.* **2020**, *20*, 3791.
[170] Y. Huang, M. Zhu, Y. Huang, Z. Pei, H. Li, Z. Wang, Q. Xue, C. Zhi, *Adv. Mater.* **2016**,

28, 8344.

[171] F. Zhao, J. Bae, X. Zhou, Y. Guo, G. Yu, *Adv. Mater.* **2018**, *30*, 1801796.

[172] Z. Wang, H. Li, Z. Tang, Z. Liu, Z. Ruan, L. Ma, Q. Yang, D. Wang, C. Zhi, *Adv. Funct. Mater.* **2018**, *28*, 1804560.

[173] H. J. Kwon, Y. Osada, J. P. Gong, *Polym. J.* **2006**, *38*, 1211.

[174] R. J. Shephard, *Energy Environ. Sci.* **2009**, *2009*, 178.

[175] Q. Fu, S. Hao, L. Meng, F. Xu, J. Yang, *ACS Nano* **2021**, *15*, 18469.

[176] X. Wang, X. Lu, B. Liu, D. Chen, Y. Tong, G. Shen, *Adv. Mater.* **2014**, *26*, 4763.

[177] C. Qin, A. Lu, *Carbohydr. Polym.* **2021**, *274*, 118667.

[178] T. Ye, J. Wang, Y. Jiao, L. Li, E. He, L. Wang, Y. Li, Y. Yun, D. Li, J. Lu, *Adv. Mater.* **2022**, *34*, 2105120.

[179] T. B. H. Schroeder, A. Guha, A. Lamoureux, G. VanRenterghem, D. Sept, M. Shtein, J. Yang, M. Mayer, *Nature* **2017**, *552*, 214.

[180] J. Kim, J. Oh, H. Lee, *Appl. Therm. Eng.* **2019**, *149*, 192.

[181] P. Yang, C. Feng, Y. Liu, T. Cheng, X. Yang, H. Liu, K. Liu, H. J. Fan, *Adv. Energy Mater.* **2020**, *10*, 2002898.

[182] D. J. Beebe, J. S. Moore, J. M. Bauer, Q. Yu, R. H. Liu, C. Devadoss, B. H. Jo, *Nature* **2000**, *404*, 588.

[183] H. Qin, T. Zhang, N. Li, H. P. Cong, S. H. Yu, *Nat. Commun.* **2019**, *10*, 1.

[184] Y. Tan, D. Wang, H. Xu, Y. Yang, X. L. Wang, F. Tian, P. Xu, W. An, X. Zhao, S. Xu, *ACS Appl. Mater. Interfaces* **2018**, *10*, 40125.

[185] L. W. Xia, R. Xie, X. J. Ju, W. Wang, Q. Chen, L. Y. Chu, *Nat. Commun.* **2013**, *4*, 2226.

[186] R. Yoshida, K. Uchida, Y. Kaneko, K. Sakai, A. Kikuchi, Y. Sakurai, T. Okano, *Nature* **1995**, *374*, 240.

[187] J. Kim, J. A. Hanna, M. Byun, C. D. Santangelo, R. C. Hayward, *Science* **2012**, *335*, 1201.

[188] C. Wang, R. J. Stewart, J. Kopecek, *Nature* **1999**, *397*, 417.

[189] D. Morales, E. Palleau, M. D. Dickey, O. D. Velev, *Soft Matter* **2014**, *10*, 1337.

[190] B. Xue, M. Qin, T. Wang, J. Wu, D. Luo, Q. Jiang, Y. Li, Y. Cao, W. Wang, *Adv. Funct. Mater.* **2016**, *26*, 9053.

[191] E. Palleau, D. Morales, M. D. Dickey, O. D. Velev, *Nat. Commun.* **2013**, *4*, 2257.

[192] Y. Osada, H. Okuzaki, H. Hori, *Nature* **1992**, *355*, 242.

[193] H. Zhu, B. Xu, Y. Wang, X. Pan, Z. Qu, Y. Mei, *Sci. Robot.* **2021**, *6*, eabe7925.

[194] Z. Shao, S. Wu, Q. Zhang, H. Xie, T. Xiang, S. Zhou, *Polym. Chem.* **2021**, *12*, 670.

[195] S. Y. Chin, Y. C. Poh, A. C. Kohler, J. T. Compton, L. L. Hsu, K. M. Lau, S. Kim, B. W. Lee, F. Y. Lee, S. K. Sia, *Sci. Robot.* **2017**, *2*, eaah6451.
[196] C. Xin, D. Jin, Y. Hu, L. Yang, R. Li, L. Wang, Z. Ren, D. Wang, S. Ji, K. Hu, D. Pan, H. Wu, W. Zhu, Z. Shen, Y. Wang, J. Li, L. Zhang, D. Wu, J. Chu, *ACS Nano* **2021**, *15*, 18048.
[197] L. J. Cheng, *Biomicrofluidics* **2018**, *12*, 021502.
[198] I. Cunha, R. Barras, P. Grey, D. Gaspar, E. Fortunato, R. Martins, L. Pereira, *Adv. Funct. Mater.* **2017**, *27*, 1606755.
[199] S. Li, J. Zheng, J. Yan, Z. Wu, Q. Zhou, L. Tan, *ACS Appl. Mater. Interfaces* **2018**, *10*, 42573.
[200] Y. Zang, F. Zhang, C. A. Di, D. Zhu, *Mater. Horiz.* **2015**, *2*, 140.
[201] A. Chortos, Z. Bao, *Mater. Today* **2014**, *17*, 321.
[202] A. N. Sokolov, M. E. Roberts, Z. Bao, *Mater. Today* **2009**, *12*, 12.
[203] Q. F. Guan, Z. M. Han, K. P. Yang, H. B. Yang, Z. C. Ling, C. H. Yin, S. H. Yu, *Nano Lett.* **2021**, *21*, 2532.
[204] G. W. King, R. M. Hainer, P. C. Cross, *Phys. Rev.* **1947**, *71*, 433.
[205] J. H. van Vleck, *Phys. Rev.* **1947**, *71*, 425.
[206] W. L. Song, Y. J. Zhang, K. L. Zhang, K. Wang, L. Zhang, L. L. Chen, Y. Huang, M. Chen, H. Lei, H. Chen, D. Fang, *Adv. Sci.* **2020**, *7*, 1902162.
[207] D. C. Hogg, F. O. Guiraud, *Nature* **1979**, *279*, 408.
[208] Y. S. Zhang, A. Khademhosseini, *Science* **2017**, *356*, eaaf3627.
[209] J. Liu, L. Mckeon, J. Garcia, S. Pinilla, S. Barwich, M. Möbius, P. Stamenov, J. N. Coleman, V. Nicolosi, *Adv. Mater.* **2022**, *34*, 2106253.
[210] G. Gao, F. Yang, F. Zhou, J. He, W. Lu, P. Xiao, H. Yan, C. Pan, T. Chen, Z. L. Wang, *Adv. Mater.* **2020**, *32*, 2004290.
[211] Y. Zhu, J. Zhang, J. Song, J. Yang, Z. Du, W. Zhao, H. Guo, C. Wen, Q. Li, X. Sui, *Adv. Funct. Mater.* **2020**, *30*, 1905493.
[212] W. Ge, S. Cao, Y. Yang, O. J. Rojas, X. Wang, *Chem. Eng. J.* **2021**, *408*, 127306.
[213] X. Sui, H. Guo, C. Cai, Q. Li, C. Wen, X. Zhang, X. Wang, J. Yang, L. Zhang, *Chem. Eng. J.* **2021**, *419*, 129478.
[214] B. Ying, R. Z. Chen, R. Zuo, J. Li, X. Liu, *Adv. Funct. Mater.* **2021**, *31*, 2104665.
[215] T. Zhu, C. Jiang, M. Wang, C. Zhu, N. Zhao, J. Xu, *Adv. Funct. Mater.* **2021**, *31*, 2102433.

[216] J. Lu, J. Gu, O. Hu, Y. Fu, D. Ye, X. Zhang, Y. Zheng, L. Hou, H. Liu, X. Jiang, *J. Mater. Chem. A* **2021**, *9*, 18406.

[217] Y. Wu, Y. Zeng, Y. Chen, C. Li, R. Qiu, W. Liu, *Adv. Funct. Mater.* **2021**, *31*, 2107202.